

# Practical considerations for enabling Li|polymer electrolyte batteries

Peter Lennartz<sup>§1</sup>, Benjamin A. Paren<sup>§2</sup>, Abraham Herzog-Arbeitman<sup>3</sup>, Xi Chelsea Chen<sup>4</sup>,  
Jeremiah A. Johnson<sup>3</sup>, Martin Winter<sup>1</sup>, Yang Shao-Horn<sup>2,5,6</sup>, Gunther Brunklaus<sup>1,7,\*</sup>

<sup>§</sup>These authors contributed equally

<sup>1</sup> Forschungszentrum Jülich GmbH, Helmholtz-Institute Münster, IEK-12, Corrensstr. 46, D-48149 Münster, Germany

<sup>2</sup> Research Laboratory of Electronics, Massachusetts Institute of Technology, 77 Massachusetts Ave, Cambridge, MA 02139, USA

<sup>3</sup> Department of Chemistry, Massachusetts Institute of Technology, 77 Massachusetts Ave, Cambridge, MA 02139, USA

<sup>4</sup> Oak Ridge National Laboratory, 5800, Oak Ridge, TN 37830, USA

<sup>5</sup> Department of Mechanical Engineering, Massachusetts Institute of Technology, 77 Massachusetts Ave, Cambridge, MA 02139, USA

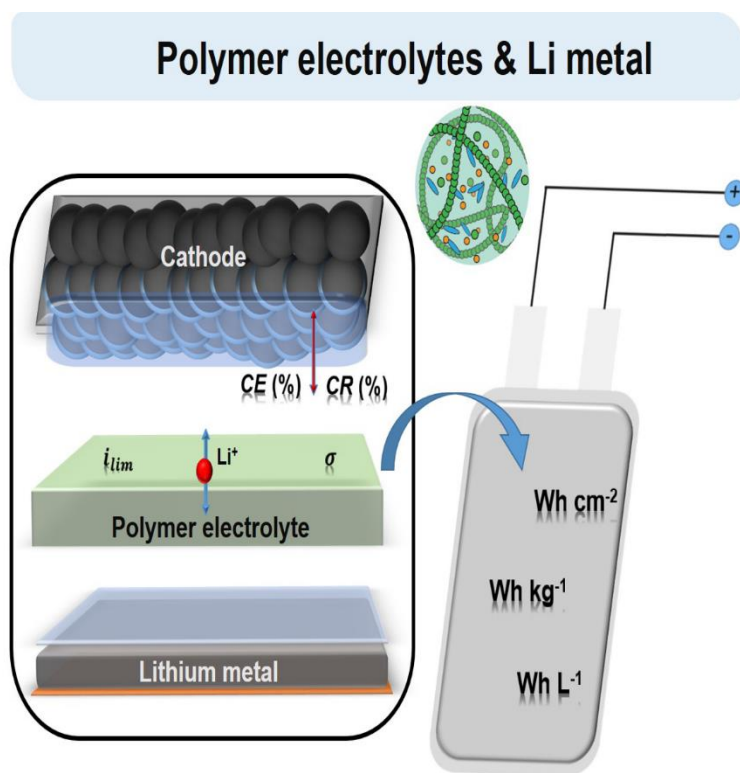
<sup>6</sup> Department of Materials Science and Engineering, Massachusetts Institute of Technology, 77 Massachusetts Ave, Cambridge, MA 02139, USA

<sup>7</sup> Lead contact

\*Correspondence: [g.brunklaus@fz-juelich.de](mailto:g.brunklaus@fz-juelich.de)

## SUMMARY

Rechargeable lithium metal batteries hold the promise to deliver high energy densities, though their commercial application is hampered by challenges such as inhomogeneous lithium deposition or capacity fading due to irreversible processes at electrode interfaces. Focusing on polymer-based electrolytes, the importance of realistic benchmarks in energy density as well as key characteristics governing the cycling reversibility of cells are thoroughly discussed, also evaluating projected energy densities of lab-scale and multi-layered pouch cells. To facilitate meaningful comparison of reported cell data, the average energy released per cycle is highlighted as a metric. In addition, the electrochemical performance of polymer-based systems is compared to liquid- and ceramic-based systems, covering recent advances while offering perspectives towards further advancement of high performance and durable energy storage applications based on lithium metal batteries.



**Keywords:** lithium metal batteries, polymer electrolytes, projected energy density, reversibility Li inventory, metrics, key cell characteristics

## INTRODUCTION

### *Polymers in lithium metal batteries – Scientific and technological milestones and potential*

There is significant interest in realizing rechargeable lithium metal batteries (LMBs) owing to promising energy densities and substantial advances in current materials development and electrode interface engineering. Substitution of typical insertion electrodes such as graphite with lithium metal requires new electrolyte materials that mitigate detrimental interfacial and interphasial side reactions upon charging and discharging.<sup>1–5</sup> While novel electrolyte materials have been introduced, challenges of sustaining reversibility of the lithium inventory upon operation remain, which motivates exploration of unprecedented electrolytes. The selection of electrolytes in systems containing Li metal is critical to the practical use of rechargeable LMBs.

### *Scientific and technological advances of polymer-based LMBs*

While early technologies of LMBs with liquid electrolytes suffered from severe reversibility and safety issues,<sup>1</sup> thus limiting their commercialization in the 1980s, recent electrolyte advances from liquid, ceramic, and polymeric materials have enabled a renaissance in LMB research and technology in the last decade (**Figure 1a**), rendering increased specific energy, cycle life and Coulombic efficiency.<sup>6–14</sup> Notably, specific energies of up to 350 Wh kg<sup>-1</sup> and cycle life of 600 have been demonstrated using a 16-layer cell stack with a liquid electrolyte and Li metal (20  $\mu$ m) vs. LiNi<sub>0.6</sub>Mn<sub>0.2</sub>Co<sub>0.2</sub>O<sub>2</sub> cathode.<sup>6</sup> In addition, energy densities of up to 900 Wh L<sup>-1</sup> are reported to be achieved using a solid-state electrolyte and Ag-C-based Li composite anode.<sup>15</sup>

These formidable advances<sup>6–12,26</sup> have catalyzed further research and development of polymer electrolytes for LMBs. Polymer electrolytes offer a variety of advantages to liquid and ceramic electrolytes, including processability, abundance and operational safety provided that their

ionic conductivity and electrochemical stability could be made comparable to the state-of-the-art electrolytes. Polymer materials are typically more processable, and form better interfaces with and within composite electrodes than ceramic systems.<sup>27–29</sup> In addition, they are adaptable and capable of incorporating dopants, fillers, or any solvents as well as tunable molecular chemistry and structure to access vast physicochemical properties. Polymer electrolytes based on polyethylene oxide (PEO), pioneered by Wright<sup>30</sup> and Armand,<sup>31</sup> have been studied extensively and are being utilized in commercial batteries.<sup>2,12,24,25</sup> Some scientific and technological advances in these electrolytes and implementation in LMBs over the past decades are highlighted in **Figure 1a**. Hydro-Quebec has pioneered Li||V<sub>2</sub>O<sub>5</sub> cells with a PEO/LiTFSI electrolyte since the 1990s, which afford a relatively high specific energy (100 – 200 Wh kg<sup>-1</sup> on a module level) and long cycle life (250 – 600 cycles).<sup>10</sup> Bolloré has further developed its “Bluecar” battery exploiting Li||LiFePO<sub>4</sub>, with a PEO-based and Li-salt-based electrolyte, for application in electric vehicles, incorporated into a 30 kWh battery pack.<sup>2,25</sup> SEEO has subsequently built and tested lithium metal batteries with NCA (nickel-cobalt-aluminum) cathodes and a nanostructured solid polymer electrolyte, enabling a specific energy of 220 Wh kg<sup>-1</sup> on the cell level when cycled at C/3 (0.25 Ah capacity).<sup>12</sup> The major advance of SEEO technology comprises the fact that these all-solid cells with lithium metal anodes for cycling and abuse testing were built using a pilot line with modified battery manufacturing equipment (such as mixers, coaters, slitters, and so on).

#### *Polymer electrolytes as flexible multi talents*

Key properties of liquid, ceramic, and dry polymer electrolytes, as well as single-ion conducting gel polymer electrolytes are shown in **Figure 1b**, extending previous comparisons from literature.<sup>27–29,32,33</sup> Liquid electrolytes exhibit excellent wetting properties, as well as high ionic

conductivity, while suffering from low mechanical stability, and potentially reduced safety. On the other hand, ceramic electrolytes provide high mechanical stability and potentially higher safety, but are incapable of electrode wetting. Polymer-based electrolytes potentially fill the gap between these contrasting properties due to their mechanical flexibility and stability, which provides great variability in the overall performance of polymer electrolytes depending on the type of system, including whether or not they operate as single-ion conductors and if they are gels (containing some liquid solvent). A key hindrance of the further development of salt-in-polymer electrolytes constitutes their limited ionic conductivity ( $\sim 10^{-4}$  S cm<sup>-1</sup> at 25°C) and Li<sup>+</sup> transference number ( $\sim 0.3$ ). While yet to be realized commercially, a promising class of polymer electrolytes in recent research include single-ion conducting gel polymer electrolytes. A single-ion conducting polymer (SIC) leads to high lithium ion transference numbers close to 1, similar to that of ceramic electrolytes, but in the dry state their conductivity remains very low.<sup>27,28</sup> However, swelling a SIC with a liquid solvent can significantly enhance the conductivity to values much closer to that of the state-of-the-art liquid electrolytes without reducing the transference number.<sup>27,28</sup> Furthermore, SIC gels maintain many of the convenient advantages of traditional salt-in-polymer electrolytes,<sup>27,28</sup> including shape flexibility, processability, and safety, though with some trade-offs. SICs just represent one new class of polymers that present alternatives to salt-in-polymer systems, and polymer electrolytes can achieve desired properties after optimization. These properties, such as conductivity and transference number, are typically evaluated in laboratory settings before implementation into battery prototypes, and are often not tested with active electrode materials. It is necessary to overcome the current challenges for polymer electrolytes in practical implementation such as limited ionic conductivity, power output, and in some cases high temperature operation.

Despite unprecedented demand for safe, durable, high-energy batteries, the LMB remains in its infancy. Innovation in new electrolytes, particularly for polymers are crucial to enable future LMB technologies. The following chapters will focus on criteria required for industrial-level implementation of polymer-based LMBs, efficient evaluation of newly introduced materials in relevant settings, and developments to date of promising polymer electrolytes for LMB systems.

## DISCUSSION

### *Challenges of evaluating polymer-based LMBs*

Evaluation of LMBs, and in particular polymer-based LMBs is not straightforward and requires careful consideration of multiple aspects, including scale of single-layer vs. multi-layer cells and relevant key parameters of the cell and individual components. In this chapter, we demonstrate how energy density can be projected from academic single-cell systems to multi-layer polymer electrolyte-based systems and briefly describe key parameters of polymer electrolytes.

### *Design considerations from academic cells to multi-layered cell stacks*

Developing advanced batteries is, in general, not only a problem of material optimization, but also requires considering a range of scales from a single cell commonly operated in research laboratories to industrially relevant stacked pouch cells. Representations of batteries at multi-cell and single-cell designs are illustrated in **Figure 2**. Key factors at the cell level are interfacial impedance, rate capability, capacity retention, and Coulombic efficiency. Key parameters at the stack level comprise cycle life, volume expansion, and energy density. At commercial-level multi-stack pouches, more prominent metrics include safety, processability, and cost per Wh kg<sup>-1</sup>. A primary challenge in battery development thus comprises the translation of scientific progress in

academic research to system (industrially relevant) level performance. Recently, Tan et al. have provided a perspective on scalability considerations and challenges for all-solid-state (ceramics based) batteries and proposed baseline protocols for cell fabrication and evaluation of pouch-type cells.<sup>34</sup>

Performance criteria on a single-cell level are typically based on high Coulombic efficiency (CE), rate capability and capacity retention (cycle life),<sup>35</sup> as well as relatively low overall interfacial/interphasial impedances.<sup>36</sup> It can be demanding to translate published results into benchmarks for recognizing ‘good’ and ‘bad’ systems due to the variety of parameters influencing the performance, and the selective lens through which certain material and cell design parameters are used. For example, a system that runs for over 1000 cycles with high Coulombic efficiency may be considered to have ‘good’ cycle life, but it is not necessarily a ‘good’ cell system if it operates with a low cathode mass loading and a thick Li anode, thereby diminishing the advantage of energy density.<sup>37</sup> Moreover, reproducibility of cell performance is especially challenging, as even minor changes in experimental procedures may have substantial impact on the Li surface (the storage conditions, manufacturer, etc.) and thus the initial conditions inside the cells.

To effectively develop LMB technologies, promising results should be both reproducible and scalable beyond individual cells. Transitioning to multi-layered cell stacks in pouch cells adds further critical metrics such as volume expansion and specific energy of the battery as well as the cost per energy (\$ per Wh), the cost of manufacturing, and safety. Economic benefits are of crucial importance for technological adaption, as the transition to extensive production of technologies such as beyond Li-ion LMBs can come with enormous investment costs.<sup>38</sup> Two parameters we present to highlight the challenge in translating from single cells to multi-cell stacks are specific energy (a performance metric) and required stack pressure for effective operation (an operating

parameter). The specific energy of a single cell is lower compared to the same chemistry in a multi-cell stack, due to double-sided electrodes and higher percentage of cell housing relative to the overall mass and volume. Additionally, the force necessary for a required stack pressure scales linearly with electrode area which means, that going from 1 cm<sup>2</sup> of a single cell to 30 cm<sup>2</sup> for a larger pouch cell (e.g. 1 Ah pouch cell<sup>3</sup>) would require a 30-fold increase in force and potentially necessitates the use of heavy steel pressure plates and screws (lowering the specific energy). Furthermore, minimizing excess lithium inventory is key to achieve high specific energy for practical devices. A specific energy of 350 Wh kg<sup>-1</sup> in a 16-layer cell stack was achieved for an LMB with a 20 µm Li anode and liquid electrolyte.<sup>6</sup> The optimum ratio of anode and cathode capacity (N/P) was found to be 1:1 in this case, where thinner lithium (lower ratio) would fail to compensate for initial Li losses and thicker lithium (higher ratio) would cause excessive SEI formation and consequently electrolyte degradation.<sup>6</sup> Thus, to advance polymer electrolytes in LMBs for practical use, further exploration of these metrics is required.

### *Projection of energy density and specific energy*

The projection of specific energy at the multi-layer cell level can be estimated with few input parameters. We show projections of both specific energy and energy density of a model battery system based on a solid electrolyte, solid-(composite)-cathode and lithium metal in **Figure 3**.

The model cell has a lithium thickness of 50 µm, electrolyte membrane thickness of 50 µm, composite cathode active mass loading of 7 mg cm<sup>-2</sup> and a cathode thickness of 65 µm. Calculation of the specific energy of a single-layered pouch cell, including all passive elements and an average reversible cycling capacity of 175 mAh g<sup>-1</sup> (based on cathode active mass loading) at 3.5 V, results



in 66 Wh kg<sup>-1</sup> (90 Wh L<sup>-1</sup>), which is below that of Li-ion batteries. For the single-layered pouch cell, the casing (100 µm pouch foil) strongly affects the energy density. Upscaling to a 15-layered pouch cell roughly doubles both specific energy and energy density (Projection I, 130 Wh kg<sup>-1</sup> and 184 Wh L<sup>-1</sup>), as the impact of the casing is reduced. Decreasing cathode mass loading, increasing cathode density as well as decreasing lithium and electrolyte layer thickness can boost the cell energy for practical applications. Adjusting the lithium thickness to 20 µm, electrolyte thickness to 25 µm, and the cathode thickness to 186 µm (20 mg cm<sup>-2</sup>) increases the specific energy to 250 Wh kg<sup>-1</sup> (392 Wh L<sup>-1</sup>, Projection II), approaching those of commercially available systems based on lithium metal and polymer electrolytes (Blue solutions), shown in **Figure 3**. Still, most targets announced by commercial manufacturers are beyond our model system Projection II. One critical parameter for solid polymer electrolyte systems represents the composite cathode, which is required to access active particles throughout the porous electrode. As such, the active mass ratio in the polymer-supported cathode drops from > 90 wt% to 60-80 wt% to provide sufficient Li-ion transport throughout the cathode,<sup>46,47</sup> thereby substantially lowering the overall specific energy. Specific energy above the United States Advanced Battery Consortium (USABC)<sup>48</sup> target of 350 Wh kg<sup>-1</sup> at the (multi-layer) cell level and C/3 is reached with Projection III, which consists of a dense and highly loaded cathode (90 % active material, 25 mg cm<sup>-2</sup> active mass loading at a thickness of 100 µm) and delivers a reversible discharge capacity of 200 mAh g<sup>-1</sup>. However, the current target of the Battery500 project<sup>49</sup> of 500 Wh kg<sup>-1</sup> on (multi-layer) cell level is not reached based on this projection.

Reversible charge/discharge capacity and operating voltage may also affect the specific energy. Since a detailed analysis is beyond the scope of this article, a ready-to-use tool is provided as a supporting file to this manuscript, which allows the inclined reader to calculate the expected

specific energy of a multilayered pouch cell with customizable parameters, such as lithium thickness and cathode active mass loading. This tool is especially relevant at early stages of academic research, when novel invented materials are sparsely available (mg scale) and only small-scale battery tests (e.g. coin cells) are feasible. An extrapolation of specific energy in multilayered pouch cells may indicate whether further adaption of the newly developed material appears meaningful and which steps should be pursued to boost the specific energy. However, this tool does not project cycling performance, which might change upon transitioning from academic coin cells to industrially more relevant multi-layered pouch cells. Adaption of this projection tool to other battery systems can be achieved with minor efforts. In the following section, the variety of performance parameters of LMBs and most important properties of polymer electrolytes are presented.

### ***Performance parameters of polymer-based LMBs and polymer electrolytes***

Beyond projection of specific energy, the evaluation of electrochemical performance is crucial to advance polymer-based LMBs. The cell performance is not only determined by external experimental conditions, but also by the design of the cell, including the mass loading of the cathode and thickness of lithium metal anode as well as the ratio of electrolyte and active material.<sup>6</sup> A wide range of cell designs, testing parameters, and polymer properties employed in published polymer-based LMB studies is illustrated in **Table 1**, and dissonance in these conditions or absence of their reporting in many studies has received increasing attention in recent publications.<sup>4,6,50–52</sup> There is a high potential for misinterpretation and misjudgment of published data in contemporary battery research of LMBs.<sup>53</sup> Relevant properties such as required operating temperature and mechanical stability are uniquely important for polymer electrolytes. While liquid electrolytes and

non-polymeric ceramic electrolytes exist in the liquid and solid state, respectively, polymer electrolytes can be semi-crystalline, glassy amorphous, in a melt state, or even swollen with a liquid solvent. Each of these states requires different considerations regarding the processing, and mechanical stability of the electrolytes, which can be dependent on temperature. Ionic conductivity and transference number of the polymer electrolyte are also extremely variable among reported studies, resulting in a significant impact on battery power and performance. Experimental conditions can vary enormously, extraction of actual performance parameters is quite challenging. In the following paragraphs, we elaborate on the characterization of key properties of polymer electrolytes, focusing on their relevance for optimization and limitations.

#### *Ionic conductivity and ionic transport*

Ionic conductivity has long been reported extensively when improving polymer electrolytes. Electrochemical impedance spectroscopy (EIS) is an established method to measure ionic conductivity of polymer electrolytes, which is determined from the measured bulk resistance and the polymer film geometry. Phase transitions, film expansion, and changes in interfacial area are all changes the polymer can experience on heating and cooling,<sup>54</sup> and strategies such as the use of spacer rings are utilized to minimize these effects, and thus these changes need to be considered and reported when testing these materials in full cells.<sup>51,52</sup> Notably, the ionic conductivity of liquid electrolytes is often determined without a separator, which slows down bulk charge transport and thus ionic conductivity.<sup>55</sup> For fair comparison between liquid and polymeric electrolytes, the more realistic conductivity of separators soaked with liquid electrolyte may be referred to. Polymer electrolytes can have high transference numbers close to 1, particularly if they are single-ion conductors, which means that the anion mobility is considerably lower compared to  $\text{Li}^+$  and

polarization effects upon charge/discharge processes are reduced.<sup>56</sup> Quantification of transference numbers is often performed based on the Bruce-Vincent-Method.<sup>57</sup> Notably, the actual quantity extracted from the Bruce-Vincent-Method is the steady-state current fraction  $\rho_+$ , which resembles the transference number only in the limit of a dilute solution where the salt activity coefficient is unity.<sup>58</sup> For reasons of uniformity and simplicity, we refer to the current fraction throughout this work as the transference number. It is important to precisely determine the initial current by setting the sampling rate high, as it changes almost instantly within tens of milliseconds, whereas current relaxation may take several hours.<sup>59</sup> Typical values of cationic transference numbers range from 0.3 (relatively mobile anions) to 1.0 (immobile anions).<sup>60,61</sup>

#### *Limiting current density*

The limiting (or sometimes critical) current density is the maximum current density sustainable in an electrolyte<sup>62</sup> and is an important parameter to be reported. As such, the critical current density (CCD) is frequently reported in the all-solid state inorganic (ceramic) electrolytes community.<sup>63,64</sup> A similar quantity is rigorously defined for a salt containing liquid or polymeric electrolyte set-up, in symmetric Li||Li cells, where concentration polarization occurs upon charging the electrolyte|electrode interface.<sup>58</sup> The limiting current density  $j_{\text{lim}}$  is reached when the anion concentration at the electrode of Li reduction converges to zero and creates a mass-transport induced depletion zone. This effect was first described by Sand in 1901 and consequently the “Sand’s time” was established, which describes the time until anion depletion likely forces onset of Li dendrite growth, if the limiting current density is applied.<sup>65</sup> This phenomenon was further explored by Chazalviel in 1990, who discovered that the protrusion growth rate of Li is equal to

the anion drift velocity.<sup>66</sup> Monroe and Newman advanced this model for the growth of Li protrusions in polymer electrolytes and defined  $j_{\text{lim}}$  as:<sup>67</sup>

$$j_{\text{lim}} = \frac{2 c_b D F}{(1 - t_+) L} \quad (1)$$

With  $c_b$  as salt concentration in the conducting phase, the apparent salt diffusion coefficient  $D$ , Faraday constant  $F$ ,  $\text{Li}^+$  transference number  $t_+$  and  $L$  distance between both electrodes. Determining the current limitations of polymer electrolytes can be done in symmetric Li||Li cells, either by galvanostatic cycling or galvano- or potentiodynamic current/voltage sweeps. In galvanostatic cycling experiments, both the shape and magnitude of the overvoltage curve correlate with interfacial stability, rendering them important criteria for evaluating artificial SEI layers. Notably, the limiting current density is particularly relevant for achieving high charge/discharge rates and thus determines the time required to charge/discharge a battery to full operational capacity. As such, high achievable Li-Polymer interfacial stability and limiting current density constitute relevant conditions to enable high-mass loading cathodes. Cycling performance, including Coulombic efficiency, is likely impaired when operating close to the limiting current density, as inhomogeneous Li deposition/dissolution occurs. Further exploring the limiting current density for polymer electrolytes is a key step in evaluating their viability for practical LMB applications.

### *Mechanical properties*

Mechanical properties are especially important when considering polymer electrolytes, as a major advantage of polymer materials compared to ceramic electrolytes is their flexibility. In addition, mechanical rigidity is considered to mitigate or limit the formation of Li dendrites by mechanical suppression. For example, the seminal work of Monroe and Newman states that

dendrites cannot occur if the modulus of Li is exceeded ( $\sim 5$  GPa) by the electrolyte.<sup>68</sup> Reaching this value with polymer materials, however, is challenging, as most polymer membranes exhibit moduli of  $0.1 - 10$  MPa.<sup>69</sup> Still, dendrite-free operation at current densities below the limiting current density is possible for polymer membranes.<sup>70</sup> Recent studies have exploited other strategies including cross-linked polymers<sup>71</sup> or SICs with low molar volumes of ions<sup>72</sup> to reduce dendrite growth, presenting possible alternatives to requiring a high modulus polymer electrolyte.

#### *Interfacial and interphasial resistance*

Interfacial/Interphasial resistance between the electrode and electrolyte is perhaps among the most important parameters that govern charge transfer and overpotentials in a cell and therefore its performance. Notably, it is seldomly reported consistently with all available data. Interfacial/Interphasial resistances are typically presented in a Nyquist plot, which shows both real and imaginary parts of electrochemical impedance at different frequencies. The resistances should be normalized to the area ( $\Omega \text{ cm}^2$ ), since the overall resistance of electrodes scales inversely with the electrode area. While liquid electrolytes typically have low interfacial/interphasial resistances ( $<100 \Omega \text{ cm}^2$ ),<sup>73</sup> solid-state ceramics may sometimes exhibit rather high interfacial/interphasial resistance ( $>100 \Omega \text{ cm}^2$ ). A benchmark value for internal resistance in all-solid-state batteries has been proposed to be around  $40 \Omega \text{ cm}^2$  for a cell in order to achieve  $5 \text{ mAh cm}^{-2}$  at a cycling rate of  $1\text{C}$ .<sup>74</sup> Polymer electrolytes have a large range of interfacial resistances in contact with electrodes, ranging from below  $100 \Omega \text{ cm}^2$  to over  $1000 \Omega \text{ cm}^2$ .<sup>75,76</sup>

#### *Coulombic efficiency*

Coulombic efficiency (CE), i.e. the amount of discharge capacity over charge capacity of an electrode, is among the most reported parameters for batteries and requires special attention in case of Li metal-based cell chemistry. This is due to the highly reactive nature of Li metal and associated interphase formation (i.e. loss of charge carriers), as well as the excess amount of Li on the anode prior to first charge.<sup>50</sup> In conventional LIBs, the cathode CE mostly represents the overall efficiency of the cells (typically there is no excess Li source in graphite), however, the source of Li ions in LMBs is less clear. It is therefore good practice to not only determine the full cell (cathode) CE, but also the Li CE, e.g. in a Li||Cu cell set-up. Suitable protocols for determining Li CE were identified for example by Adams et al. that consider irregularities from different Cu substrate surface conditions.<sup>77</sup> Quantifying Li CE is especially relevant for developing future polymer-based cells, as it is crucial for enabling thin Li excess anodes and cells with larger energy densities.

Another key bottleneck of polymer electrolytes comprises the cell performance and designs. Electrolytes with high conductivities may not be effective if charge transfer at electrode interfaces is slow. Similarly, while cycling performance at room-temperature for more than 1000 cycles is impressive, it may be weak if thin cathodes and thick anodes were exploited. The next section will compare in more detail frequently used metrics to evaluate polymer electrolytes for LMB, and propose a new metric to meaningfully evaluate these systems.

### ***Recent advances in polymer-based LMBs and how to evaluate them***

Coulombic efficiency, energy efficiency, cycle life, capacity retention, and interfacial/interphasial resistances are key parameters to evaluate LMBs. As previously discussed, the ionic conductivity and transference number of the polymer electrolyte are also extremely

variable among reported studies and can contribute to battery performance. The wide range of these properties for a variety of polymer electrolytes in LMBs reported is shown in **Figure 4**, including salt-in-polymer electrolytes (pure polymer + salt<sup>25,75,76,78–81</sup>, polymer + salt composite<sup>60,82–85</sup>, and gels<sup>86–92</sup>) and single-ion conductors (dry systems<sup>93–95</sup> and gels<sup>61,96–110</sup>), and gels, respectively. Most of the LMB-polymer systems identified in the literature contained LiFePO<sub>4</sub> (LFP) as cathode material, some systems were presented with higher capacity active material such as LiNi<sub>x</sub>Mn<sub>y</sub>Co<sub>z</sub>O<sub>2</sub> (NMC) or LiCoO<sub>2</sub> (LCO). Details of each reference can be found in Table S2 in the Supporting Information. The electrochemical properties presented in **Figure 4** show no clear favorable active cathode material, thus it is not highlighted further. A larger data set could potentially enable further insights in the future.

Ionic conductivity and transference number do not seem to be correlated (**Figure 4a**), though it can be seen that most salt-in-polymer systems are operated above 30 °C, whereas many of the SICs are operated at room temperature and show similar ionic conductivity ranges. However, nearly all of the SICs are blended with some kind of solvent, which leads to the high conductivities at room temperature. The highest room-temperature conductivity seen in the reported SIC gels is  $\sim 1.5 \times 10^{-3} \text{ S cm}^{-1}$  (polymers 38<sup>104</sup> and 39<sup>105</sup> in **Figure 4**) are both based on a network type lithium bis(allylmalonato)borate (LiBAMB) and pentaerythritol tetrakis(2-mercaptoacetate) polymer. Some gel-based polymer-in-salt systems, such as, polymer 21<sup>90</sup> (a cellulose/PEO composite with added LiTFSI in DMSO), can achieve a room temperature conductivity higher than  $10^{-3} \text{ S cm}^{-1}$ , though transference number is typically below 0.6. A comparison of CE (averaged over the published cycle life of the cells) in LMBs with active cathode materials, and the fraction of Li<sup>+</sup> conductivity (the conductivity multiplied with transference number) is displayed in **Figure 4b**. There is no clear trend between CE and Li<sup>+</sup> conductivity,



though we note that the SICs appear to have higher CE in general compared to the salt-in-polymer system, partially reflecting higher electrochemical stability that has been reported for SICs.

Higher Coulombic efficiency exists in the systems with the longest cycle life, as seen in **Figure 4c**, where materials with higher CE are able to last for more cycles prior to failure. However, in most studies, the batteries are not cycled until failure, so it is possible that many of the polymer systems could last much longer than their reported cycle life, or the authors may have selected to stop reporting immediately before significant capacity losses might occur. Similarly, the capacity retention decreases as the number of cycles increases (**Figure 4d**), which is expected due to regular capacity losses and CE of <100 %. To better understand the full capabilities of the electrolytes in LMBs, additional insight could be gained if more studies reported capacity retention until a defined failure point, such as for example  $C_{\text{initial}}/2$ . Reporting in this manner could also prevent selective reporting of high CE's from just a small number of cycles, as mentioned in Chapter 2. There appears to be no clear trend for the relation between interfacial/interphasial resistances of polymer electrolytes in contact with Li and liquid uptake, **Figure 4e**. Operation temperature indicates that it may be beneficial for room temperature operation to add liquid components, (though more data should be gathered to support such trends). We note that interfacial/interphasial resistances and liquid uptake (for gels) are often unreported, and inclusion of this data could significantly strengthen the assessment of polymers as effective electrolytes.

There is no electrolyte that clearly excels in more than one or two of the parameters included in **Figure 4**. For example, the boron-based network gel SIC previously discussed (polymers 38<sup>104</sup> and 39<sup>105</sup>) may have excellent conductivity and transference number (**Figure 4a**), but the capacity retention and number of cycles are more towards the center of the distribution of systems examined (**Figure 4d**). Alternatively, polymers 35 (a polyimide based SIC polymer

electrolyte<sup>102</sup> ) and 44 (an electrospun nanofiber *es*-PVPSI membrane with EC/DMC<sup>110</sup>) have some of the highest CE and cycle life (1000 cycles, **Figure 4c**), but this appears to be at the expense of lower conductivity compared to polymers 38 and 39 (**Figure 4a**). This significant variety in properties, which are often used to characterize ‘good’ or ‘bad’ polymer electrolytes for LMBs highlights the necessity for improved methods of translating from published data to actual battery performance.

### *Identifying “good” and “bad” systems*

Early considerations in the late 1990s included the ‘energy throughput’ of batteries, which describes the total energy released during cycling life,<sup>112</sup> and the lithium figure of merit,<sup>113</sup> which was defined as accumulated discharge capacity at the end of a cycle divided by the theoretical capacity of the complete Li inventory in both anode and cathode. Risse et al. described several figures of merit for Li-Sulfur (Li-S) cells, where the average capacity of the Li-S battery was calculated based on the total accumulated charge output divided by the number of cycles at which half of the initial capacity was reached.<sup>114</sup> Here, we propose a related metric, the average energy released per cycle:

$$\text{Av. energy released per cycle} = \frac{C_{\text{initial}} + C_{\text{final}}}{2} \cdot V_{\text{nominal}} \cdot m_{\text{act}} \quad (2),$$

where  $C_{\text{initial}}$  and  $C_{\text{final}}$  denote the initial and final specific discharge capacities (in mAh g<sup>-1</sup>),  $V_{\text{nominal}}$  is the nominal voltage, and  $m_{\text{act}}$  is the active mass loading of the cathode (in mg cm<sup>-2</sup>); please see **Figure S1** for further details (Supporting Information).

The total energy of the cell was calculated as the average energy per cycle multiplied by the number of reported cycles). The energy per cycle is presented in units of Wh cm<sup>-2</sup> and not Wh L<sup>-1</sup> or Wh kg<sup>-1</sup>, as the overall specific energy and energy density including all passive components

(such as cell casing) was not available for almost all publications. Average power is calculated by multiplying the average energy per cycle with the C-rate, in that way punishes slow charging rates. Indeed, the proposed metric offers several advantages compared to conventional comparison of data (typically based on cycling number and C-rate, or those metrics included in **Figure 4**). The average capacity and operational (or nominal) voltage are, when combined, more meaningful to describe the actual amount of energy stored in a cell per gram of active mass, and multiplication with the active mass punishes the use of low (and unfavorable) mass loadings and in turn rewards higher mass loadings. Furthermore, normalization of the energy to the electrode area by multiplication with mass loading is independent on the type of battery and can be scaled up to estimate the actual specific energy (in Wh kg<sup>-1</sup>) of individual cells or cell stacks with variable weight fractions of passive components (including casings). Since the technological adaption of novel electrolytes in multi-layered cells cannot be performed at early stages of development, this metric reflects a compromise between academic practicality (leaving out explicit calculations of the energy density of multi-layered cell stacks) and technological relevance (expressing performance in terms of energy density). We note that a key limitation of this metric is the fact that it penalizes systems with high cycle number, because  $C_{final}$  is typically lower after a larger number of cycles. However, this could be addressed in future studies by reporting the average energy per cycle after a standard number of cycles (i.e. 100, 200, 300, ...), for a more equitable comparison. **Figure 5a** compares the reported average Coulombic efficiency with the average energy released per cycle in LMBs with a variety of types of electrolytes, with a comparison of Coulombic efficiency and total energy (average energy released \* number of cycles) found in **Figure 5b**, as well as average power (**Figure 5c**).

We compare the polymer electrolyte systems (index 1-44, discussed in **Figure 4**) to two LMBs with liquid electrolytes,<sup>6,7</sup> two solid-state electrolytes with a Li-metal anode,<sup>13,14</sup> a solid-state electrolyte with a  $\mu$ Si-type anode,<sup>8</sup> and a hybrid ceramic/liquid/polymer electrolyte (a cellulose based aerogel, with LLZO nanowires and  $\text{LiPF}_6$  in EC/DMC), which we refer to as the CGE (composite gel electrolyte).<sup>115</sup> The cells with liquid<sup>6,7,115</sup> and solid-state<sup>8,13,14</sup> electrolytes are able to release much more energy than the considered polymer electrolytes while still maintaining high Coulombic efficiency. Among the polymer electrolytes examined, there is not a clear correlation between Coulombic efficiency, and energy released per cycle. Polymers 34 and 44 (both SIC gels with LFP cathodes) demonstrate comparatively high total energy and average power, likely due to their high cathode mass loadings compared to the other polymer-based systems. The references containing liquid/solid state electrolytes show higher power density than most of the polymer systems, potentially indicating their capability of higher charge/discharge rates. As there are multiple variables involved, more studies may need to be done to elucidate specific trends of power.

Overall, the findings strongly suggest that the energy output of LMBs with polymer electrolytes must be improved (while still maintaining high Coulombic efficiency and cycle life), in order to become potentially competitive with liquid and solid-state electrolytes.

#### *Toward higher cathode mass loadings*

The cathode mass loadings of the liquid, solid-state, and CGE electrolytes are all higher than those in case of the polymer electrolytes reported in **Figure 5**, which in part leads to the high energy outputs. Cells that comprise thick cathodes with high mass loadings exhibit challenges for the polymer electrolyte to fully access all the Li inventory, and thus limit energy density. On the

other hand, systems with liquid electrolytes may benefit from straightforward infiltration of electrolyte into the cathode, or in case of the demonstrated  $\mu\text{Si}$ -solid-state system, involve processing of the inorganic electrolyte with the active NMC materials.<sup>8</sup> The lack of data indicates that polymers may not be as compatible with mass loadings  $>20 \text{ mg cm}^{-2}$ , but it is also possible that such high cathode loadings have not been prioritized upon testing with many of these materials. While we have specifically used this to highlight the energy released from LMBs with polymer electrolytes, this approach could be more broadly applied to other types of liquid and solid-state electrolytes as well. We note that the presented cathode Coulombic efficiency is an average value based on the available data, other representations of cycling efficiency, such as accumulated Coulombic efficiency,<sup>111</sup> could not be extracted from most literature references.

#### *Stack pressure matters*

It is important to establish additional metrics to more broadly evaluate polymer-based LMBs for their suitability for practical usage. For example, stack pressure is an important external factor that influences Li plating morphology, cyclability and propensity to form Li dendrites. Increasing the stack pressure in liquid electrolyte based cells can yield improved Li cyclability.<sup>116–118</sup> While the optimum stack pressure for liquid electrolyte cells is dependent on the types of liquid electrolyte and separator used, Dahn et al. have reported that an applied pressure of 75 kPa was sufficient to sustain 95 % capacity retention at 50 cycles in a dual-salt lithium difluoro(oxalato)borate ( $\text{LiDFOB}$ )/ $\text{LiBF}_4$  liquid electrolyte based ‘anode-free’ cell.<sup>118</sup> In a polymer electrolyte-based Li battery consisting of a PEO/ $\text{LiTFSI}$  electrolyte and Li metal, the interfacial/interphasial impedance between the polymer electrolyte and Li anode decreases by 1-2 orders of magnitude with increasing stack pressure up to 400 and 200 kPa at 60 and 80 °C,

respectively.<sup>119</sup> In comparison to liquid and polymer-based cells, high stack pressure is required for oxide and sulfide electrolytes to ensure contact between the solid electrolyte and the electrodes and minimize void evolution. Sakamoto et al. have investigated the effect of stack pressure on the Li plating and stripping through LLZO solid electrolyte.<sup>120</sup> A ‘critical stack pressure’ is needed to enable effective Li plating and stripping, below which dramatic increases in the cell potential was observed. The ‘critical stack pressure’ increased with increasing current density, from 0.4 MPa at 0.1 mA cm<sup>-2</sup> to 2.0 MPa at 0.4 mA cm<sup>-2</sup>.<sup>120</sup> Meng et al. have discovered that a minimum stack pressure of 5 MPa allows for reliable Li plating and stripping through the argyrodite-type solid electrolyte Li<sub>6</sub>PS<sub>5</sub>Cl.<sup>121</sup> Many academic studies invoked much higher stack pressures than these reported minimum values to mitigate challenges at the solid electrolyte|electrode interfaces. For polymer electrolytes, much lower stack pressure is needed to form sufficiently good contact at the polymer|electrode interface, though it is worth noting that investigations of the effect of stack pressure on Li plating/stripping through polymer electrolytes are scarce. Further measurements and reporting of stack pressure in polymer-based LMBs would be beneficial for better understanding of their potential for practical applications.

### *Safety and sustainability*

Additionally, seldomly reported criteria comprise safety and sustainability (e.g. ‘green chemistry’) of lithium metal-based systems. The lack of reporting of these criteria may also be due to less quantifiability of such parameters. Common safety experiments include flammability tests, flexibility tests and piercing or cutting of cell stacks. Here, polymer electrolytes can be beneficial for safety in LMBs, as they potentially enable flexible cell stacks and may consist of flame-retardant materials.<sup>122</sup> Regarding sustainability, materials and their production have to be

reasonably affordable and environmentally acceptable (e.g. abundant, non-toxic), rendering efforts for recycling as crucial source of materials necessary, particularly to establish a trade-off between using materials of high value (high recycling potential) and materials that are rather abundant (low recycling potential). In the following (and last) chapter, explicit polymer design considerations are presented, highlighting the most recent advances in the development of polymer electrolytes for LMBs.

### ***Design considerations for the next generation of polymer electrolytes for LMBs***

As the technical requirements for viable polymer LMBs come into greater focus, several directions have been proposed to take advantage of the substantial chemical tunability, interfacial compatibility, and high safety of polymer electrolyte materials, while also increasing conductivity, transference number, and general stability in LMB settings. However, the vastness of the polymer design space necessitates focus in experimental efforts. When practically infinite polymer chemistries can be accessed in many architectures, eventually doped with any number of solvents, nanoparticles, or other additives, experimenter time becomes the limiting factor. Progress towards an industrially viable LMB requires cognizance of many performance requirements simultaneously. With this in mind, we highlight several trends that show exciting promise to further advance the design of polymer electrolytes for lithium metal batteries: aggregates for decoupled ion transport, addition of molecular and ionic dopants for phase separated nanochannels, and network polymer structures (**Figure 6**).

The use of polymer materials has long been proposed to mechanically discourage Li dendrite growth in response to electrode volume changes or uneven lithium deposition through a combination of interfacial compatibility and viscoelastic resistance to cracking. However, many

of the most conductive coupled systems are essentially viscous liquids,<sup>123</sup> that may risk cell leakage and are unlikely to depress dendrite formation. Balsara and coworkers have demonstrated the great promise of all-solid-state polymer electrolytes, particularly block copolymers of conductive and glassy monomers, which are highly effective at maintaining structural durability while achieving ionic conductivities comparable to homopolymers of their conductive block.<sup>124</sup> These materials, including both single-ion conducting and salt-in-polymer systems, cannot only supply high transference numbers essential for lithium dendrite suppression, but can also demonstrate tunable modulus, yield strength, and adhesion to electrodes, all of which are salient to dendrite suppression.<sup>70,124–127</sup> These approaches have been effective in increasing cell lifetime in thin films based on LiF in microporous polymers<sup>72</sup> as well as plasticized semicrystalline polyethylene/PEO networks.<sup>71</sup>

#### *Decoupled ionic transport*

Attempts to decouple ionic conductivity from any structural relaxation to benefit from a more inorganic-like ion hopping conduction mechanism as advised by Sokolov<sup>128–130</sup> and Winey<sup>131–133</sup> have advanced to include dedicated ion-channels in dry SIC polymers, in which the large ionic aggregates can quickly transfer ions via exchanging counterions in their corresponding solvation shells. Ionic aggregates are also common in polymer-in-salt electrolyte systems. Liu et al. present a polymer-in-salt system featuring a micro-structured electrode material which displays excellent conductivity, cycling, rate, and safety characteristics.<sup>134</sup> Jones et al. show an ionic conductivity comparable to PEO in self-assembled zwitterionic assemblies when LiTFSI is added, with transference numbers above 0.5 due to the sluggish dynamics of larger TFSI anions through the dense ionic channels.<sup>135</sup> This conductivity is shown to be superionic and localized in the



ordered ionic aggregate phase, though investigations of electrochemical stability and exploitation in full galvanic cells are not provided. These results are similar to previous decoupled salt-filled neutral polymers based on highly rigid phosphine sulfide monomers,<sup>136</sup> but the transference numbers and full cell performance remain unknown. Polyanions like PSTFSI-Li<sup>94</sup>, and a-TFSI-Li analogs<sup>137–140</sup> incorporating PEO as a block copolymer or blend, as well as other chemistries exhibit reasonably good mechanical properties resulting from microphase separation while demonstrating promising electrochemical performance in LMBs. Transference numbers are high (~0.9) in accordance with their single-ion character but the achievable ionic conductivity is still somewhat coupled to the segmental dynamics in the conductive phase, limiting application in batteries to elevated operating temperatures. More efforts for the investigation of highly decoupled ion-aggregating materials in LMBs appears warranted.

#### *Molecular and ionic dopants*

Adding molecular and ionic dopants has recently been shown to facilitate nanophase separated channels for improved transport properties. Such channels can form in previously discussed SIC gels, which in many cases have a polar phase of ions and solvents to facilitate ion transport, with a nonpolar backbone phase to add mechanical stability.<sup>103–109</sup> Addition of suitable amounts of structural solvent enabled room-temperature operation of gel polymer electrolytes based on a sulfonamide backbone.<sup>98,141</sup> An alternative approach was recently taken by Yang et al., in which Cu(II) and Li salts were added to expand the fibrillar structure of oxygen-rich natural polymers such as cellulose for decoupled lithium transport.<sup>26</sup> Cu<sup>2+</sup> cations are shown to move sluggishly in these Li-Cu-cellulose nanofibril (CNF) materials, but play an integral role in loosening the fibril bundle to allow reversible lithium infiltration and hopping. By blending this

material into an LFP cathode and casting a film as an electrolyte, an LMB showed relatively stable cycling performance with 94 % capacity retention over 200 cycles and reasonable performance with high voltage LMO and NMC cathodes. Similar materials have since then been invoked as hydroxide conductors for fuel cell applications.<sup>142</sup>

Notably, ~2 % water and ~5-10 % ethylene carbonate are present in the material in bound form. Water should be generally avoided in LMBs due to its reactivity with Li metal. Also, the leakage, flammability, and toxicity risks associated with carbonates, other bulk organic solvents, and gel polymer electrolytes that may contain them have motivated a push towards all-solid systems. However, it is clear that the remarkable performance of this system is predicated on these small molecule additives and it is likely that the properties and stabilities of these species are moderated by the salts and the polymer hosts, similar to effects observed in solvate ionic liquids (SILs) which display high electrochemical stability and miniscule vapor pressure despite nominally containing small molecule ‘solvents’.<sup>143</sup> As the Li-Cu-CNF material demonstrates, mechanical properties are not compromised by this solvent, though additional investigation on its safety is necessary. Thus, while truly dry highly conductive polymer electrolytes have been a longstanding goal of the field, a transformational technology such as a viable LMB must be prioritized. It seems likely that the next generation of polymer electrolyte materials will contain small molecule plasticizers or dopants, whether they act as bulk solvents or not, while still maintaining operational safety.

### *In-situ polymerization*

Another promising approach to high-performance electrolytes takes advantage of in situ polymerization or crosslinking of small molecules to produce polymer (network) membranes with

exceptional wetting of the electrode materials and high conductivity. These membranes may be plasticized by residual monomer and oligomeric species after crosslinking, or may contain other additives such as ionic liquids,<sup>144</sup> deep eutectic solvents (DES)<sup>145</sup> or others, thereby decoupling ionic conductivity from the relaxation of the polymer network and creating largely vehicular transport. By virtue of the in-situ solidification process, the liquid precursor infiltrates the cathode materials, ensuring excellent interfacial compatibility of the resulting electrolyte membrane. When properly designed, these materials typically are nonflammable, do not leak, and show strong ability of Li dendrite suppression. High-performing membranes have been reported, using dioxolane (DOL) polymerization in conjunction with poly-dopamine in a PVdF-HFP matrix.<sup>146</sup> This class of materials affords excellent cycling stability over 800 cycles even at 2C, losing just 0.021 % capacity per cycle on average. Hydrogen bonding between poly-dopamine and dioxolane within the PVdF-HFP host creates a robust network structure with good mechanical properties and excellent wetting and Li dendrite suppression, enabling pouch cells to function even when cut. Similar strategies have shown promise with poly(vinylethylene carbonate) membranes,<sup>147</sup> cross-linked polyTHF materials which show weaker Li<sup>+</sup> binding and higher transference numbers,<sup>148</sup> and lignin particle-derived branched polymers.<sup>149</sup>

### *Polymers as artificial interphases*

Besides being utilized as electrolytes, polymers can serve as engineered interphasial layers between Li metal (or current collector) and solid or liquid electrolytes to promote rather uniform Li deposition/stripping while preventing side reactions. As such, polymers can also take the role of an artificial SEI to improve interfacial contacts, Li compatibility, and reversibility of the Li inventory. Several design strategies have been proposed. Bao et al. have introduced a series of

polyurethane-based soft and flowable polymers as an interphasial layer between Li metal and liquid electrolytes to improve Li cyclability and reversibility of the Li inventory.<sup>150,151</sup> Guo et al. have fabricated a lithium polyacrylate (LiPAA) layer with high elasticity which can stretch up to 580 % to accommodate Li deformation during plating/stripping processes and reduce Li dendrite growth.<sup>152</sup> Kang et al. have shown that PVdF (polyvinylidene difluoride) as interphasial layer with high dielectric constant can promote uniform Li deposition.<sup>153</sup> The polymer layer can also be applied underneath Li or current collector. It's been demonstrated that the polymer layer underneath the current collector can effectively reduce the plating stress, thereby avoiding stress-driven dendrite growth.<sup>154</sup> We note that understanding SEI chemistry and engineering of an ideal SEI is of crucial importance for all types of batteries,<sup>155,156</sup> and especially challenging in case of Li metal due to its reactive and dynamic nature.<sup>157</sup> While specific benchmarks for properties such as mechanical stability or exchange current densities of SEI layers are yet to be identified, an ideal SEI should exhibit both high and uniform Li conduction, as well as thermodynamic stability.<sup>158</sup> A combination of advanced characterization techniques and simulation is likely required to develop mechanistic understanding of SEI formation and deposition/dissolution processes.<sup>158</sup> Wu et al. recently demonstrated how simulation and theoretical prediction of the SEI constituents derived from poly- $\epsilon$ -caprolactone-based polymer electrolytes in contact with Li metal anodes could potentially contribute to more knowledge-driven development of polymer electrolytes, that is exploiting the complex interplay and reactivity of degradation products on the Li metal surface.<sup>159</sup>

Given the many performance requirements of solid and pseudo-solid electrolytes in LMBs, it is perhaps unsurprising that the complexity of such materials is increasing, including multiple polymer chemistries or architectures, small molecule dopants, additional salts, and inorganic particles to increase electrochemical stability, decoupling, durability, or wettability. While these

additions often boost the demands and difficulty of material synthesis, particularly on scales of industrial relevance, a modular approach of tackling performance requirements one at a time, each with a dedicated material component, has proven fruitful. Whether or not such modularity persists in the field, rigorous testing is clearly key to reproducible, comparable, and transferable results. This motivates interest in high-throughput automation and machine learning based approaches, where experimental efforts by humans can be streamlined as much as possible. Whatever the approach, the ability of polymer electrolytes to form thin, durable, highly-wetting layers should be retained, as these traits are important to the rate capability and cycling stability of LMBs.

## **CONCLUSION AND OUTLOOK**

Polymer-based electrolytes offer unique opportunities to combine mechanical strength and shape flexibility with sufficient charge carrier transport. However, despite substantial research efforts, challenges regarding reversibility of the Li inventory and achievable energy density remain. Extrapolation of academic cells to multi-layer pouch cells impressively demonstrates the importance of realistic benchmarks: even with optimized film thickness, advances in achieving higher cathode mass loadings and reversible discharge capacity are required to meet industrial demands. Evaluation of electrochemical cell performance and material properties is prone to misinterpretation, not least due to the high dependence on the test conditions and large variation thereof. Instead of conventional evaluation of systems based on transport properties (e.g. ionic conductivity) and performance properties (e.g. discharge capacity), a new metric is proposed, that denotes the average accessible energy per cycle. This metric includes cathode mass loadings and operating voltage and shows a system's potential to be considered for larger scales. An outlook on the latest advances in material development illustrates the ever-increasing complexity of developed

materials, including multiple polymer chemistries and small dopants. The future of polymer electrolytes in lithium metal batteries can most likely be predicted by strongly focusing on their main advantages: high versatility and straight-forward processability. Hybrid combinations with inorganic solid or liquid electrolytes are reasonable cases, where polymers either can act as both flexible and mechanically robust components, or can stabilize interfaces towards anode and cathode, respectively.

## **ACKNOWLEDGMENTS**

This work was funded by the US-German collaboration on ‘Interfaces and Interphases in Rechargeable Li-metal based Batteries’, as part of the joint research project ‘LISI’ by the U.S. Department of Energy (DOE) and the Federal Ministry of Education and Research (BMBF). P.L., G.B. and M.W. kindly acknowledge support by the German Federal Ministry of Education and Research (BMBF: grants 13XP0224A, 13XP0509A). B.A.P. and Y. S. H. kindly acknowledge the support of the Assistant Secretary for Energy Efficiency and Renewable Energy, Office of Vehicle Technologies of the U.S. Department of Energy under Contract No. DE-AC02-06CH11357 under the Advanced Battery Materials Research (BMR) Program and the US-Germany Cooperation on Energy Storage. This work was supported in part by the Toyota Research Institute. The authors thank Professor Nitash Balsara for fruitful discussions on the conceptualization of this work.

## **AUTHOR CONTRIBUTIONS**

Concept, P.L., B.A.P., G.B., and Y.S.H.; Writing – Original Draft, P.L., B.A.P., A.H.A., and X.C.C; Writing – Review & Editing, G.B., Y.S.H., and M.W., Supervision, G.B., Y.S.H, J.A.J., and M.W.

## DECLARATION OF INTERESTS

The authors declare no competing interests.

## REFERENCES

1. Winter, M., Barnett, B., and Xu, K. (2018). Before Li Ion Batteries. *Chem. Rev.* *118*, 11433–11456. 10.1021/acs.chemrev.8b00422.
2. Nair, J.R., Imholt, L., Brunklaus, G., and Winter, M. (2019). Lithium Metal Polymer Electrolyte Batteries: Opportunities and Challenges. *Electrochem. Soc. Interface* *28*, 55–61. 10.1149/2.F05192if.
3. Chen, S., Niu, C., Lee, H., Li, Q., Yu, L., Xu, W., Zhang, J.-G., Dufek, E.J., Whittingham, M.S., Meng, S., et al. (2019). Critical Parameters for Evaluating Coin Cells and Pouch Cells of Rechargeable Li-Metal Batteries. *Joule* *3*, 1094–1105. 10.1016/j.joule.2019.02.004.
4. Liu, J., Bao, Z., Cui, Y., Dufek, E.J., Goodenough, J.B., Khalifah, P., Li, Q., Liaw, B.Y., Liu, P., Manthiram, A., et al. (2019). Pathways for practical high-energy long-cycling lithium metal batteries. *Nat. Energy* *4*, 180–186. 10.1038/s41560-019-0338-x.
5. Hobold, G.M., Lopez, J., Guo, R., Minafra, N., Banerjee, A., Meng, Y.S., Shao-Horn, Y., and Gallant, B.M. (2021). Moving beyond 99.9% Coulombic Efficiency for Lithium Anodes in Liquid Electrolytes. *Nat. Energy* *6*, 951–960. 10.1038/s41560-021-00910-w.
6. Niu, C., Liu, D., Lochala, J.A., Anderson, C.S., Cao, X., Gross, M.E., Xu, W., Zhang, J.G., Whittingham, M.S., and Xiao (2021). Balancing Interfacial Reactions to Achieve Long Cycle Life in High-Energy Lithium Metal Batteries. *Nat. Energy* *6*, 723–732. 10.1038/s41560-021-00852-3.
7. Xue, W., Huang, M., Li, Y., Zhu, Y.G., Gao, R., Xiao, X., Zhang, W., Li, S., Xu, G., and Yu, Y. (2021). Ultra-High-Voltage Ni-Rich Layered Cathodes in Practical Li Metal Batteries Enabled by a Sulfonamide-Based Electrolyte. *Nat. Energy* *6*, 495–505. 10.1038/s41560-021-00792-y.
8. Tan, D.H.S., Chen, Y.-T., Yang, H., Bao, W., Sreenarayanan, B., Doux, J.-M., Li, W., Lu, B., Ham, S.-Y., and Sayahpour (2021). Carbon-Free High-Loading Silicon Anodes Enabled by Sulfide Solid Electrolytes. *Science* *373*, 1494–1499. 10.1126/science.abg7217.
9. QuantumScape White Paper, A deep dive into QuantumScape's fast charging performance, QuantumScape (2022). <https://www.quantumscape.com>.
10. Takeda, Y., Imanishi, N., and Yamamoto, O. (2009). Developments of the Advanced All-Solid-State Polymer Electrolyte Lithium Secondary Battery. *Electrochem.* *77*, 784–797. 10.5796/electrochemistry.77.784.
11. Chen, Y.-H., Lennartz, P., Liu, K.L., Hsieh, Y.-C., Scharf, F., Guerdelli, R., Buchheit, A., Grünebaum, M., Kempe, F., Winter, M., et al. (2023). Towards all-solid-state polymer batteries: going beyond PEO with hybrid concepts, *Adv. Funct. Mater.* *2300501*. 10.1002/adfm.202300501.
12. Eitouni, H., Yang, J., Pratt, R., Wang, X.-L., and Grape, U. (2015). Final Technical Report High-Voltage Solid Polymer Batteries for Electric Drive Vehicles.
13. Cronk, A., Chen, Y.-T., Deysher, G., Ham, S.-Y., Yang, H., Ridley, P., Sayahpour, B., Nguyen, L.H.B., Oh, J.A.S., and Jang, J. (2023). Overcoming the Interfacial Challenges of LiFePO<sub>4</sub> in Inorganic All-Solid-State Batteries. *ACS Energy Lett.* *8*, 827–835. 10.1021/acsenenergylett.2c02138.
14. Zhang, Z., Chen, S., Yang, J., Wang, J., Yao, L., Yao, X., Cui, P., and Xu, X. (2018). Interface Re-Engineering of Li<sub>10</sub>GeP<sub>2</sub>S<sub>12</sub> Electrolyte and Lithium anode for All-Solid-State Lithium Batteries with Ultralong Cycle Life. *ACS Appl. Mat. Int.* *10*, 2556–2565. 10.1021/acsaami.7b16176.
15. Lee, Y.-G., Fujiki, S., Jung, C., Suzuki, N., Yashiro, N., Omoda, R., Ko, D.-S., Shiratsuchi, T., Sugimoto, T., and Ryu, S. (2020). High-Energy Long-Cycling All-Solid-State Lithium Metal Batteries Enabled by Silver–Carbon Composite Anodes. *Nat. Energy* *5*, 299–308. 10.1038/s41560-020-0575-z.
16. Armand, M. (1983). Polymer Solid Electrolytes - an Overview. *Solid State Ion.* *9–10*, 745–754. 10.1016/0167-2738(83)90083-8.
17. Bates, J.B., Dudney, N.J., Gruzalski, G.R., Zuh, R.A., Choudhury, A., Luck, C.F., and Robertson, J.D. (1993). Fabrication and Characterization of Amorphous Lithium Electrolyte Thin Films and Rechargeable Thin-Film Batteries. *J. Power Sources* *43*, 102–110. 10.1016/0378-7753(93)80106-Y.
18. Soo, P.P., Huang, B., Jang, Y., Chiang, Y., Sadoway, D.R., and Mayes, A.M. (1999). Rubbery Block Copolymer Electrolytes for Solid-State Rechargeable Lithium Batteries. *J. Electrochem. Soc.* *146*, 32–37. 10.1149/1.1391560.
19. Yamada, Y., and Yamada, A. (2015). Superconcentrated Electrolytes for Lithium Batteries. *J. Electrochem. Soc.* *162*, 2406–2423. 10.1149/2.0041514jes.
20. Yu, Z., Wang, H., Kong, X., Huang, W., Tsao, Y., Mackanic, D.G., Wang, K., Wang, X., Huang, W., and Choudhury, S. (2020). Molecular Design for Electrolyte Solvents Enabling Energy-Dense and Long-Cycling Lithium Metal Batteries. *Nat. Energy* *5*, 526–533. 10.1038/s41560-020-0634-5.
21. Pereira, N., Amatucci, G.G., Whittingham, M.S., and Hamlen, R. (2015). Lithium–Titanium Disulfide Rechargeable Cell Performance after 35 Years of Storage. *J. Power Sources* *280*, 18–22. 10.1016/j.jpowsour.2015.01.056.
22. Py, M.A., and Haering, R.R. (1983). Structural Destabilization Induced by Lithium Intercalation in MoS<sub>2</sub> and Related Compounds. *Can. J. Phys.* *61*, 76–84. 10.1139/p83-013.
23. Reddy, M.V., Mauger, A., Julien, C.M., Paoletta, A., and Zaghib, K. (2020). Brief History of Early Lithium-Battery Development. *Materials* *13*, 1884. 10.3390/ma13081884.
24. Wilkinson, H., and Cornay, S. (2005). Avestor Lithium-Metal-Polymer Batteries Deployed throughout North America. In *INT'EL EC 05 - Twenty-Seventh International Telecommunications Conference*, IEEE, pp. 217–221. 10.1109/INTLEEC.2005.335095.
25. Hovington, P., Lagacé, M., Guerfi, A., Bouchard, P., Mauger, A., Julien, C.M., Armand, M., and Zaghib, K. (2015). New Lithium Metal Polymer Solid State Battery for an Ultrahigh Energy: Nano C-LiFePO<sub>4</sub> versus Nano Li<sub>1.2</sub>V<sub>3</sub>O<sub>8</sub>. *Nano Lett.* *15*, 2671–2678. 10.1021/acs.nanolett.5b00326.

26. Yang, C., Wu, Q., Xie, W., Zhang, X., Brozena, A., Zheng, J., Garaga, M.N., Ko, B.H., Mao, Y., and He, S. (2021). Copper-Coordinated Cellulose Ion Conductors for Solid-State Batteries. *Nature* 598, 590–596. 10.1038/s41586-021-03885-6.
27. Gao, J., Wang, C., Han, D.-W., and Shin, D.-M. (2021). Single-Ion Conducting Polymer Electrolytes as a Key Jigsaw Piece for next-Generation Battery Applications. *Chem. Sci.* 12, 13248–13272. 10.1039/D1SC04023E.
28. Deng, K., Zeng, Q., Wang, D., Liu, Z., Qiu, Z., Zhang, Y., Xiao, M., and Meng, S.Y. (2020). Single-Ion Conducting Gel Polymer Electrolytes: Design. *Prep. Appl. J. Mater. Chem. A* 8, 1557–1577. 10.1039/C9TA11178F.
29. Cekic-Laskovic, I., Wölke, C., Xu, K., and Winter, M. (2021). Electrolytes: From a Thorn Comes a Rose, and from a Rose, a Thorn. *Isr. J. Chem.* 61, 85–93. 10.1002/ijch.202000102.
30. Wright, P.V. (1975). Electrical Conductivity in Ionic Complexes of Poly(Ethylene Oxide). *Br. Polym. J.* 7, 319–327. 10.1002/pi.4980070505.
31. Armand, M. (1994). The History of Polymer Electrolytes. *Solid State Ion.* 69, 309–319. 10.1016/0167-2738(94)90419-7.
32. Brandell, D., Mindemark, J., and Hernández, G. (2021). Polymer-Based Solid-State Batteries (Walter de Gruyter GmbH & Co KG).
33. Cekic-Laskovic, I., Aspern, N., Imholt, L., Kaymaksiz, S., Oldiges, K., Rad, B.R., and Winter, M. (2017). Synergistic Effect of Blended Components in Nonaqueous Electrolytes for Lithium Ion Batteries. *Top Curr. Chem.* 375, 37, 10.1007/s41061-017-0125-8.
34. Tan, D.H.S., Meng, Y.S., and Jang, J. (2022). Scaling up High-Energy-Density Sulfidic Solid-State Batteries: A Lab-to-Pilot Perspective. *Joule* 6, 1755–1769. 10.1016/j.joule.2022.07.002.
35. Qian, J., Henderson, W.A., Xu, W., Bhattacharya, P., Engelhard, M., Borodin, O., and Zhang, J.-G. (2015). High Rate and Stable Cycling of Lithium Metal Anode. *Nat. Commun.* 6, 6362. 10.1038/ncomms7362.
36. Xia, S., Wu, X., Zhang, Z., Cui, Y., and Liu, W. (2019). Practical Challenges and Future Perspectives of All-Solid-State Lithium-Metal Batteries. *Chem.* 5, 753–785. 10.1016/j.chempr.2018.11.013.
37. Betz, J., Bieker, G., Meister, P., Placke, T., Winter, M., and Schmich, R. (2019). Theoretical versus Practical Energy: A Plea for More Transparency in the Energy Calculation of Different Rechargeable Battery Systems. *Adv. Energy Mater.* 9, 1803170. 10.1002/aenm.201803170.
38. Duffner, F., Kronmeyer, N., Tübke, J., Leker, J., Winter, M., and Schmich, R. (2021). Post-Lithium-Ion Battery Cell Production and Its Compatibility with Lithium-Ion Cell Production Infrastructure. *Nat. Energy* 6, 123–134. 10.1038/s41560-020-00748-8.
39. Battery Technology. Blue Solutions. <https://www.blue-solutions.com/en/battery-technology/>.
40. Tesla 4680 Cell. Battery Design. <https://www.batterydesign.net/tesla-4680-cell/>.
41. Licerion Products. Sion Power. <https://sionpower.com/products/>.
42. SolidPower. <https://www.solidpowerbattery.com/>.
43. Battery World Recap. SES. <https://ses.ai/us-battery-world-2021/>.
44. ProLogium Debuts Its Next-Generation Solid-State Battery Technologies at the 2022 Paris Motor Show. Battery News. <https://batteriesnews.com/prologium-debuts-next-generation-solid-state-battery-technologies-2022-paris-motor-show/>.
45. Factorial announces 40 Ah solid-state cells. Electrive. <https://www.electrive.com/2021/04/22/factorial-announces-40-ah-solid-state-cells/>.
46. Keller, M., Varzi, A., and Passerini, S. (2018). Hybrid Electrolytes for Lithium Metal Batteries. *J. Power Sources* 392, 206–225. 10.1016/j.jpowsour.2018.04.099.
47. Al-Salih, H., Houache, M.S.E., Baranova, E.A., and Abu-Lebdeh, Y. (2022). Composite Cathodes for Solid-State Lithium Batteries: “Catholytes” the Underrated Giants. *Adv. Energy Sustain. Res.* 3, 2200032. 10.1002/aesr.202200032.
48. United States Advanced Battery Consortium. <https://uscar.org/usabc/>.
49. Battery 500: Progress Update. DOE Office of Energy Efficiency & Renewable Energy. <https://www.energy.gov/eere/articles/battery500-progress-update>.
50. Xiao, J., Li, Q., Bi, Y., Cai, M., Dunn, B., Glossmann, T., Liu, J., Osaka, T., Sugiura, R., and Wu, B. (2020). Understanding and Applying Coulombic Efficiency in Lithium Metal Batteries. *Nat. Energy* 5, 561–568. 10.1038/s41560-020-0648-z.
51. Sahore, R., Du, Z., Chen, X.C., Hawley, W.B., Westover, A.S., and Dudney, N.J. (2021). Practical Considerations for Testing Polymer Electrolytes for High-Energy Solid-State Batteries. *ACS Energy Lett.* 6, 2240–2247. 10.1021/acsenenergylett.1c00810.
52. Tikekar, M.D., Choudhury, S., Tu, Z., and Archer, L.A. (2016). Design Principles for Electrolytes and Interfaces for Stable Lithium-Metal Batteries. *Nat. Energy* 1, 16114. 10.1038/nenergy.2016.114.
53. Johansson, P., Alvi, S., Ghorbanzade, P., Karlsmo, M., Loaiza, L., Thangavel, V., Westman, K., and Årén, F. (2021). Ten Ways to Fool the Masses When Presenting Battery Research\*\*. *Batter. Supercaps.* 4, 1785–1788. 10.1002/batt.202100154.
54. Stolz, L., Homann, G., Winter, M., and Kasnatscheew, J. (2021). Area Oversizing of Lithium Metal Electrodes in Solid-State Batteries: Relevance for Overvoltage and Thus Performance? *Chem. Sus. Chem.* 14, 2163–2169. 10.1002/cssc.202100213.
55. Kirchhöfer, M., Zamory, J., Paillard, E., and Passerini, S. (2014). Separators for Li-Ion and Li-Metal Battery Including Ionic Liquid Based Electrolytes Based on the TFSI- and FSI- Anions. *Int. J. Mol. Sci.* 15, 14868–14890. 10.3390/ijms150814868.
56. Borzutzki, K., Nair, J.R., Winter, M., and Brunklaus, G. (2022). Does Cell Polarization Matter in Single-Ion Conducting Electrolytes? *ACS Appl Mater Interfaces* 14, 5211–5222. 10.1021/acsami.1c19097.
57. Bruce, P.G., and Vincent, C.A. (1987). Steady State Current Flow in Solid Binary Electrolyte Cells. *J. Electroanal. Chem. Interfacial Electrochem.* 225, 1–17. 10.1016/0022-0728(87)80001-3.
58. Frenck, L., Sethi, G.K., Maslyn, J.A., and Balsara, N.P. (2019). Factors That Control the Formation of Dendrites and Other Morphologies on Lithium Metal Anodes. *Front Energy Res.* 7, 10.3389/fenrg.2019.00115.
59. Galluzzo, M.D., Maslyn, J.A., Shah, D.B., and Balsara, N.P. (2019). Ohm’s Law for Ion Conduction in Lithium and beyond-Lithium Battery Electrolytes. *J. Chem. Phys.* 151, 020901. 10.1063/1.5109684.
60. Boaretto, N., Bittner, A., Brinkmann, C., Olsowski, B.-E., Schulz, J., Seyfried, M., Vezzù, K., Popall, M., and Noto, V. (2014). Highly Conducting 3D-Hybrid Polymer Electrolytes for Lithium Batteries Based on Siloxane Networks and Cross-Linked Organic Polar Interphases. *Chem. Mater.* 26, 6339–6350. 10.1021/cm5024647.
61. Nguyen, H.-D., Kim, G.-T., Shi, J., Paillard, E., Judeinstein, P., Lyonard, S., Bresser, D., and Iojoiu, C. (2018). Nanostructured Multi-Block Copolymer Single-Ion Conductors for Safer High-Performance Lithium Batteries. *Energy Env. Sci.* 11, 3298–3309. 10.1039/C8EE02093K.
62. Shah, D.B., Kim, H.K., Nguyen, H.Q., Srinivasan, V., and Balsara, N.P. (2019). Comparing Measurements of Limiting Current of Electrolytes with Theoretical Predictions up to the Solubility Limit. *J. Phys. Chem. C* 123, 23872–23881. 10.1021/acs.jpcc.9b07121.
63. Lu, Y., Zhao, C., Yuan, H., Cheng, X., Huang, J., and Zhang, Q. (2021). Critical Current Density in Solid-State Lithium Metal Batteries: Mechanism, Influences, and Strategies. *Adv. Funct. Mater.* 31, 2009925. 10.1002/adfm.202009925.
64. Sarkar, S., and Thangadurai, V. (2022). Critical Current Densities for High-Performance All-Solid-State Li-Metal Batteries: Fundamentals, Mechanisms, Interfaces, Materials, and Applications. *ACS Energy Lett.* 7, 1492–1527. 10.1021/acsenenergylett.2c00003.



65. Sand, H.J.S., III (1901). On the Concentration at the Electrodes in a Solution, with Special Reference to the Liberation of Hydrogen by Electrolysis of a Mixture of Copper Sulphate and Sulphuric Acid. *Lond. Edinb. Dublin Philos. Mag. J. Sci.* *1*, 45–79. 10.1080/14786440109462590.
66. Chazalviel, J.-N. (1990). Electrochemical Aspects of the Generation of Ramified Metallic Electrodeposits. *Phys. Rev. A* *42*, 7355–7367. 10.1103/PhysRevA.42.7355.
67. Monroe, C., and Newman, J. (2003). Dendrite Growth in Lithium/Polymer Systems. *J. Electrochem. Soc.* *150*, 1377. 10.1149/1.1606686.
68. Monroe, C., and Newman, J. (2005). The Impact of Elastic Deformation on Deposition Kinetics at Lithium/Polymer Interfaces. *J. Electrochem. Soc.* *152*, A396. 10.1149/1.1850854.
69. Li, J., Cai, Y., Wu, H., Yu, Z., Yan, X., Zhang, Q., Gao, T.Z., Liu, K., Jia, X., and Bao, Z. (2021). Polymers in Lithium-Ion and Lithium Metal Batteries. *Adv. Energy Mater.* *11*, 2003239. 10.1002/aenm.202003239.
70. Barai, P., Higa, K., and Srinivasan, V. (2017). Lithium Dendrite Growth Mechanisms in Polymer Electrolytes and Prevention Strategies. *Phys. Chem. Chem. Phys.* *19*, 20493–20505. 10.1039/C7CP03304D.
71. Khurana, R., Schaefer, J.L., Archer, L.A., and Coates, G.W. (2014). Suppression of Lithium Dendrite Growth Using Cross-Linked Polyethylene/Poly(Ethylene Oxide) Electrolytes: A New Approach for Practical Lithium-Metal Polymer Batteries. *J. Am. Chem. Soc.* *136*, 7395–7402. 10.1021/ja502133j.
72. Fu, C., Venturi, V., Kim, J., Ahmad, Z., Ells, A.W., Viswanathan, V., and Helms, B.A. (2020). Universal Chemomechanical Design Rules for Solid-Ion Conductors to Prevent Dendrite Formation in Lithium Metal Batteries. *Nat. Mater.* *19*, 758–766. 10.1038/s41563-020-0655-2.
73. Boyle, D.T., Kong, X., Pei, A., Rudnicki, P.E., Shi, F., Huang, W., Bao, Z., Qin, J., and Cui, Y. (2020). Transient Voltammetry with Ultramicroelectrodes Reveals the Electron Transfer Kinetics of Lithium Metal Anodes. *ACS Energy Lett.* *5*, 701–709. 10.1021/acsenenergylett.0c00031.
74. Randau, S., Weber, D.A., Kötz, O., Koerver, R., Braun, P., Weber, A., Ivers-Tiffée, E., Adermann, T., Kulisch, J., and Zeier, W.G. (2020). Benchmarking the Performance of All-Solid-State Lithium Batteries. *Nat. Energy* *5*, 259–270. 10.1038/s41560-020-0565-1.
75. Chai, J., Liu, Z., Ma, J., Wang, J., Liu, X., Liu, H., Zhang, J., Cui, G., and Chen, L. (2017). In Situ Generation of Poly (Vinylene Carbonate) Based Solid Electrolyte with Interfacial Stability for LiCoO<sub>2</sub> Lithium Batteries. *Adv. Sci.* *4*, 1600377. 10.1002/advs.201600377.
76. Zhang, H., Chen, F., Lakuntza, O., Oteo, U., Qiao, L., Martínez-Ibañez, M., Zhu, H., Carrasco, J., Forsyth, M., and Armand, M. (2019). Suppressed Mobility of Negative Charges in Polymer Electrolytes with an Ether-Functionalized Anion. *Angew. Chem. Int. Ed.* *58*, 12070–12075. 10.1002/anie.201905794.
77. Adams, B.D., Zheng, J., Ren, X., Xu, W., and Zhang, J. (2018). Accurate Determination of Coulombic Efficiency for Lithium Metal Anodes and Lithium Metal Batteries. *Adv. Energy Mater.* *8*, 1702097. 10.1002/aenm.201702097.
78. Wei, Z., Chen, S., Wang, J., Wang, Z., Zhang, Z., Yao, X., Deng, Y., and Xu, X. (2018). Superior Lithium Ion Conduction of Polymer Electrolyte with Comb-like Structure via Solvent-Free Copolymerization for Bipolar All-Solid-State Lithium Battery. *J. Mater. Chem. Mater.* *6*, 13438–13447. 10.1039/C8TA04477E.
79. Martínez-Ibañez, M., Sánchez-Diez, E., Qiao, L., Zhang, Y., Judez, X., Santiago, A., Aldalur, I., Carrasco, J., Zhu, H., and Forsyth, M. (2020). Unprecedented Improvement of Single Li-Ion Conductive Solid Polymer Electrolyte Through Salt Additive. *Adv. Funct. Mater.* *30*, 2000455. 10.1002/adfm.202000455.
80. Wang, C., Wang, T., Wang, L., Hu, Z., Cui, Z., Li, J., Dong, S., Zhou, X., and Cui, G. (2019). Differentiated Lithium Salt Design for Multilayered PEO Electrolyte Enables a High-Voltage Solid-State Lithium Metal Battery. *Adv. Sci.* *6*, 1901036. 10.1002/advs.201901036.
81. Chiou, M.-H., Borzutzki, K., Thienenkamp, J.H., Mohrhardt, M., Liu, K.-L., Mereacre, V., Binder, J.R., Ehrenberg, H., Winter, M., and Brunklaus, G. (2022). Durable Fast-Charging Lithium Metal Batteries Designed with Cross-Linked Polymer Electrolytes and Niobate-Coated Cathode. *J. Power Sources* *538*, 231528. 10.1016/j.jpowsour.2022.231528.
82. Zhou, B., Jo, Y.H., Wang, R., He, D., Zhou, X., Xie, X., and Xue, Z. (2019). Self-Healing Composite Polymer Electrolyte Formed via Supramolecular Networks for High-Performance Lithium-Ion Batteries. *J. Mater. Chem. Mater.* *7*, 10354–10362. 10.1039/C9TA01214A.
83. Tang, W., Tang, S., Guan, X., Zhang, X., Xiang, Q., and Luo, J. (2019). High-Performance Solid Polymer Electrolytes Filled with Vertically Aligned 2D Materials. *Adv. Funct. Mater.* *29*, 1900648. 10.1002/adfm.201900648.
84. Huo, H., Chen, Y., Luo, J., Yang, X., Guo, X., and Sun, X. (2019). Rational Design of Hierarchical “Ceramic-in-Polymer” and “Polymer-in-Ceramic” Electrolytes for Dendrite-Free Solid-State Batteries. *Adv. Energy Mater.* *9*, 1804004. 10.1002/aenm.201804004.
85. Wu, H., Xu, Y., Ren, X., Liu, B., Engelhard, M.H., Ding, M.S., El-Khoury, P.Z., Zhang, L., Li, Q., and Xu, K. (2019). Polymer-in-“Quasi-Ionic Liquid” Electrolytes for High-Voltage Lithium Metal Batteries. *Adv. Energy Mater.* *9*, 1902108. 10.1002/aenm.201902108.
86. Kaneko, F., Wada, S., Nakayama, M., Wakihara, M., Koki, J., and Kuroki, S. (2009). Capacity Fading Mechanism in All Solid-State Lithium Polymer Secondary Batteries Using PEG-Borate/Aluminate Ester as Plasticizer for Polymer Electrolytes. *Adv. Funct. Mater.* *19*, 918–925. 10.1002/adfm.200800789.
87. Jie, J., Liu, Y., Cong, L., Zhang, B., Lu, W., Zhang, X., Liu, J., Xie, H., and Sun, L. (2020). High-Performance PVDF-HFP Based Gel Polymer Electrolyte with a Safe Solvent in Li Metal Polymer Battery. *J. En. Chem.* *49*, 80–88. 10.1016/j.jechem.2020.01.019.
88. Dong, T., Zhang, J., Xu, G., Chai, J., Du, H., Wang, L., Wen, H., Zang, X., Du, A., and Jia, Q. (2018). Multifunctional Polymer Electrolyte Enables Ultra-Long Cycle-Life in a High-Voltage Lithium Metal Battery. *Energy Env. Sci.* *11*, 1197–1203. 10.1039/C7EE03365F.
89. Liu, X., Ding, G., Zhou, X., Li, S., He, W., Chai, J., Pang, C., Liu, Z., and Cui, G. (2017). An Interpenetrating Network Poly(Diethylene Glycol Carbonate)-Based Polymer Electrolyte for Solid State Lithium Batteries. *J. Mater. Chem. Mater.* *5*, 11124–11130. 10.1039/C7TA02423A.
90. Zhao, L., Fu, J., Du, Z., Jia, X., Qu, Y., Yu, F., Du, J., and Chen, Y. (2019). High-Strength and Flexible Cellulose/PEG Based Gel Polymer Electrolyte with High Performance for Lithium Ion Batteries. *J. Memb. Sci.* *593*, 117428. 10.1016/j.memsci.2019.117428.
91. Wu, H., Cao, Y., Su, H., and Wang, C. (2018). Tough Gel Electrolyte Using Double Polymer Network Design for the Safe, Stable Cycling of Lithium Metal Anode. *Angew. Chem. Int. Ed.* *57*, 1361–1365. 10.1002/anie.201709774.
92. Chen, Y., Hsieh, Y., Liu, K.L., Wichmann, L., Thienenkamp, J.H., Choudhary, A., Bedrov, D., Winter, M., and Brunklaus, G. (2022). Green Polymer Electrolytes Based on Polycaprolactones for Solid-State High-Voltage Lithium Metal Batteries. *Macromol. Rapid Commun.* *43*, 2200335. 10.1002/marc.202200335.
93. Porcarelli, L., Aboudzadeh, M.A., Rubatat, L., Nair, J.R., Shaplov, A.S., Gerbaldi, C., and Mecerreyes, D. (2017). Single-Ion Triblock Copolymer Electrolytes Based on Poly(Ethylene Oxide) and Methacrylic Sulfonamide Blocks for Lithium Metal Batteries. *J. Power Sources* *364*, 191–199. 10.1016/j.jpowsour.2017.08.023.

94. Bouchet, R., Maria, S., Meziane, R., Aboulaich, A., Lienafa, L., Bonnet, J.-P., Phan, T.N.T., Bertin, D., Gigmes, D., and Devaux, D. (2013). Single-Ion BAB Triblock Copolymers as Highly Efficient Electrolytes for Lithium-Metal Batteries. *Nat. Mater.* *12*, 452–457. 10.1038/nmat3602.
95. Lu, F., Li, G., Yu, Y., Gao, X., Zheng, L., and Chen, Z. (2020). Zwitterionic Impetus on Single Lithium-Ion Conduction in Solid Polymer Electrolyte for All-Solid-State Lithium-Ion Batteries. *Chem Eng J* *384*, 123237. 10.1016/j.cej.2019.123237.
96. Chen, Y., Xu, G., Liu, X., Pan, Q., Zhang, Y., Zeng, D., Sun, Y., Ke, H., and Cheng, H. (2018). A Gel Single Ion Conducting Polymer Electrolyte Enables Durable and Safe Lithium Ion Batteries via Graft Polymerization. *RSC Adv.* *8*, 39967–39975. 10.1039/C8RA07557C.
97. Porcarelli, L., Shaplov, A.S., Bella, F., Nair, J.R., Mecerreyes, D., and Gerbaldi, C. (2016). Single-Ion Conducting Polymer Electrolytes for Lithium Metal Polymer Batteries That Operate at Ambient Temperature. *ACS Energy Lett.* *1*, 678–682. 10.1021/acsenenergylett.6b00216.
98. Borzutzki, K., Thienenkamp, J., Diehl, M., Winter, M., and Brunklaus, G. (2019). Fluorinated Polysulfonamide Based Single Ion Conducting Room Temperature Applicable Gel-Type Polymer Electrolytes for Lithium Ion Batteries. *J. Mater. Chem. Mater.* *7*, 188–201. 10.1039/C8TA08391F.
99. Ji, P.-Y., Fang, J., Zhang, Y.-Y., Zhang, P., and Zhao, J.-B. (2017). Novel Single Lithium-Ion Conducting Polymer Electrolyte Based on Poly(Hexafluorobutyl Methacrylate- Co- Lithium Allyl Sulfonate) for Lithium-Ion Batteries. *Chem. Electro. Chem.* *4*, 2352–2358. 10.1002/celc.201700256.
100. Pan, Q., Chen, Y., Zhang, Y., Zeng, D., Sun, Y., and Cheng, H. (2016). A Dense Transparent Polymeric Single Ion Conductor for Lithium Ion Batteries with Remarkable Long-Term Stability. *J. Power Sources* *336*, 75–82. 10.1016/j.jpowsour.2016.10.033.
101. Chen, Y., Ke, H., Zeng, D., Zhang, Y., Sun, Y., and Cheng, H. (2017). Superior Polymer Backbone with Poly(Arylene Ether) over Polyamide for Single Ion Conducting Polymer Electrolytes. *J. Memb. Sci.* *525*, 349–358. 10.1016/j.memsci.2016.12.011.
102. Du, D., Hu, X., Zeng, D., Zhang, Y., Sun, Y., Li, J., and Cheng, H. (2020). Water-Insoluble Side-Chain-Grafted Single Ion Conducting Polymer Electrolyte for Long-Term Stable Lithium Metal Secondary Batteries. *ACS Appl. Energy Mater.* *3*, 1128–1138. 10.1021/acsaem.9b02180.
103. Cao, C., Li, Y., Feng, Y., Peng, C., Li, Z., and Feng, W. (2019). A Solid-State Single-Ion Polymer Electrolyte with Ultrahigh Ionic Conductivity for Dendrite-Free Lithium Metal Batteries. *Energy Storage Mater.* *19*, 401–407. 10.1016/j.ensm.2019.03.004.
104. Deng, K., Qin, J., Wang, S., Ren, S., Han, D., Xiao, M., and Meng, Y. (2018). Effective Suppression of Lithium Dendrite Growth Using a Flexible Single-Ion Conducting Polymer Electrolyte. *Small* *14*, 1801420. 10.1002/sml.201801420.
105. Deng, K., Wang, S., Ren, S., Han, D., Xiao, M., and Meng, Y. (2017). Network Type Sp<sup>3</sup> Boron-Based Single-Ion Conducting Polymer Electrolytes for Lithium Ion Batteries. *J. Power Sources* *360*, 98–105. 10.1016/j.jpowsour.2017.06.006.
106. Shin, D., Bachman, J.E., Taylor, M.K., Kamcev, J., Park, J.G., Ziebel, M.E., Velasquez, E., Jarenwattananon, N.N., Sethi, G.K., and Cui, Y. (2020). A Single-Ion Conducting Borate Network Polymer as a Viable Quasi-Solid Electrolyte for Lithium Metal Batteries. *Adv. Mater.* *32*, 1905771. 10.1002/adma.201905771.
107. Cao, P.-F., Li, B., Yang, G., Zhao, S., Townsend, J., Xing, K., Qiang, Z., Vogiatzis, K.D., Sokolov, A.P., and Nanda, J. (2020). Elastic Single-Ion Conducting Polymer Electrolytes: Toward a Versatile Approach for Intrinsically Stretchable Functional Polymers. *Macromolecules* *53*, 3591–3601. 10.1021/acs.macromol.9b02683.
108. Chen, Z., Steinle, D., Nguyen, H.-D., Kim, J.-K., Mayer, A., Shi, J., Paillard, E., Jojoiu, C., Passerini, S., and Bresser, D. (2020). High-Energy Lithium Batteries Based on Single-Ion Conducting Polymer Electrolytes and Li[Ni<sub>0.8</sub>Co<sub>0.1</sub>Mn<sub>0.1</sub>]O<sub>2</sub> Cathodes. *Nano Energy* *77*, 105129. 10.1016/j.nanoen.2020.105129.
109. Qin, B., Liu, Z., Ding, G., Duan, Y., Zhang, C., and Cui, G. (2014). A Single-Ion Gel Polymer Electrolyte System for Improving Cycle Performance of LiMn<sub>2</sub>O<sub>4</sub> Battery at Elevated Temperatures. *Electrochim. Acta* *141*, 167–172. 10.1016/j.electacta.2014.07.004.
110. Li, C., Qin, B., Zhang, Y., Varzi, A., Passerini, S., Wang, J., Dong, J., Zeng, D., Liu, Z., and Cheng, H. (2019). Single-Ion Conducting Electrolyte Based on Electrospun Nanofibers for High-Performance Lithium Batteries. *Adv. Energy Mater.* *9*, 1803422. 10.1002/aenm.201803422.
111. Holtstiege, F., Wilken, A., Winter, M., and Placke, T. (2017). Running out of Lithium? A Route to Differentiate between Capacity Losses and Active Lithium Losses in Lithium-Ion Batteries. *Phys. Chem. Chem. Phys.* *19*, 25905–25918. 10.1039/C7CP05405J.
112. Friedrich, R., and Richter, G. (1999). Performance Requirements of Automotive Batteries for Future Car Electrical Systems. *J. Power Sources* *78*, 4–11. 10.1016/S0378-7753(99)00004-X.
113. Hayashi, K., Nemoto, Y., Tobishima, S., and Yamaki, J. (1999). Mixed Solvent Electrolyte for High Voltage Lithium Metal Secondary Cells. *Electrochim. Acta* *44*, 2337–2344. 10.1016/S0013-4686(98)00374-0.
114. Risse, S., Angioletti-Uberti, S., Dzubiella, J., and Ballauff, M. (2014). Capacity Fading in Lithium/Sulfur Batteries: A Linear Four-State Model. *J. Power Sources* *267*, 648–654. 10.1016/j.jpowsour.2014.05.076.
115. Ding, C., Fu, X., Li, H., Yang, J., Lan, J., Yu, Y., Zhong, W., and Yang, X. (2019). An Ultrarobust Composite Gel Electrolyte Stabilizing Ion Deposition for Long-Life Lithium Metal Batteries. *Adv. Funct. Mater.* *29*, 1904547. 10.1002/adfm.201904547.
116. Wilkinson, D.P., Blom, H., Brandt, K., and Wainwright, D. (1991). Effects of Physical Constraints on Li Cyclability. *J. Power Sources* *36*, 517–527. 10.1016/0378-7753(91)80077-B.
117. Hirai, T., Yoshimatsu, I., and Yamaki, J. (1994). Influence of Electrolyte on Lithium Cycling Efficiency with Pressurized Electrode Stack. *J. Electrochem. Soc.* *141*, 611–614. 10.1149/1.2054778.
118. Weber, R., Genovese, M., Louli, A.J., Hames, S., Martin, C., Hill, I.G., and Dahn, J.R. (2019). Long Cycle Life and Dendrite-Free Lithium Morphology in Anode-Free Lithium Pouch Cells Enabled by a Dual-Salt Liquid Electrolyte. *Nat. Energy* *4*, 683–689. 10.1038/s41560-019-0428-9.
119. Gupta, A., Kazyak, E., Craig, N., Christensen, J., Dasgupta, N.P., and Sakamoto, J. (2019). Evaluating the Effects of Temperature and Pressure on Li/PEO-LiTFSI Interfacial Stability and Kinetics. *J. Electrochem. Soc.* *165*, 2801–2806. 10.1149/2.090181jes.
120. Wang, M.J., Choudhury, R., and Sakamoto, J. (2019). Characterizing the Li-Solid-Electrolyte Interface Dynamics as a Function of Stack Pressure and Current Density. *Joule* *3*, 2165–2178. 10.1016/j.joule.2019.06.017.
121. Doux, J., Nguyen, H., Tan, D.H.S., Banerjee, A., Wang, X., Wu, E.A., Jo, C., Yang, H., and Meng, Y.S. (2020). Stack Pressure Considerations for Room-Temperature All-Solid-State Lithium Metal Batteries. *Adv. Energy Mater.* *10*, 1903253. 10.1002/aenm.201903253.
122. Bai, L., Ghiassinejad, S., Brassinne, J., Fu, Y., Wang, J., Yang, H., Vlad, A., Minoia, A., Lazzaroni, R., and Gohy, J.-F. (2021). High Salt-Content Plasticized Flame-Retardant Polymer Electrolytes. *ACS Appl. Mater. Interfaces* *13*, 44844–44859. 10.1021/acsaami.1c11058.
123. Hooper, R., Lyons, L.J., Mapes, M.K., Schumacher, D., Moline, D.A., and West, R. (2001). Highly Conductive Siloxane Polymers. *Macromolecules* *34*, 931–936. 10.1021/ma001844e.

124. Rojas, A.A., Inceoglu, S., Mackay, N.G., Thelen, J.L., Devaux, D., Stone, G.M., and Balsara, N.P. (2015). Effect of Lithium-Ion Concentration on Morphology and Ion Transport in Single-Ion-Conducting Block Copolymer Electrolytes. *Macromolecules* 48, 6589–6595. 10.1021/acs.macromol.5b01193.
125. Stone, G.M., Mullin, S.A., Teran, A.A., Hallinan, D.T., Minor, A.M., Hexemer, A., and Balsara, N.P. (2012). Resolution of the Modulus versus Adhesion Dilemma in Solid Polymer Electrolytes for Rechargeable Lithium Metal Batteries. *J. Electrochem. Soc.* 159, 222–227. 10.1149/2.030203jes.
126. Patel, V., Maslyn, J.A., Chakraborty, S., Sethi, G.K., Villaluenga, I., and Balsara, N.P. (2021). Interplay between Mechanical and Electrochemical Properties of Block Copolymer Electrolytes and Its Effect on Stability against Lithium Metal Electrodes. *J. Electrochem. Soc.* 168, 120546, 10.1149/1945-7111.429.
127. Chakraborty, S., Sethi, G.K., Frenck, L., Ho, A.S., Villaluenga, I., Wantanabe, H., and Balsara, N.P. (2022). Effect of Yield Stress on Stability of Block Copolymer Electrolytes against Lithium Metal Electrodes. *ACS Appl. Energy. Mater.* 5, 852–861. 10.1021/acs.aem.1c03288.
128. Wang, Y., Agapov, A.L., Fan, F., Hong, K., Yu, X., Mays, J., and Sokolov, A.P. (2012). Decoupling of Ionic Transport from Segmental Relaxation in Polymer Electrolytes. *Phys. Rev. Lett.* 108, 088303. 10.1103/PhysRevLett.108.088303.
129. Wang, Y., and Sokolov, A.P. (2015). Design of Superionic Polymer Electrolytes. *Curr. Opin. Chem. Eng.* 7, 113–119. 10.1016/j.coche.2014.09.002.
130. Wang, Y., Fan, F., Agapov, A.L., Saito, T., Yang, J., Yu, X., Hong, K., Mays, J., and Sokolov, A.P. (2014). Examination of the Fundamental Relation between Ionic Transport and Segmental Relaxation in Polymer Electrolytes. *Polym. Guildf.* 55, 4067–4076. 10.1016/j.polymer.2014.06.085.
131. Paren, B.A., Häußler, M., Rathenow, P., Mecking, S., and Winey, K.I. (2022). Decoupled Cation Transport within Layered Assemblies in Sulfonated and Crystalline Telechelic Polyethylenes. *Macromolecules* 55, 2813–2820. 10.1021/acs.macromol.2c00132.
132. Paren, B.A., Thurston, B.A., Neary, W.J., Kendrick, A., Kennemur, J.G., Stevens, M.J., Frischknecht, A.L., and Winey, K.I. (2020). Percolated Ionic Aggregate Morphologies and Decoupled Ion Transport in Precise Sulfonated Polymers Synthesized by Ring-Opening Metathesis Polymerization. *Macromolecules* 53, 8960–8973. 10.1021/acs.macromol.0c01906.
133. Yan, L., Hauler, M., Bauer, J., Mecking, S., Winey, K.I., Haussler, M., Bauer, J., Mecking, S., and Winey, K.I. (2019). Monodisperse and Telechelic Polyethylenes Form Extended Chain Crystals with Ionic Layers. *Macromolecules* 52, 4949–4956. 10.1021/acs.macromol.9b00962.
134. Liu, W., Yi, C., Li, L., Liu, S., Gui, Q., Ba, D., Li, Y., Peng, D., and Liu, J. (2021). Designing Polymer-in-Salt Electrolyte and Fully Infiltrated 3D Electrode for Integrated Solid-State Lithium Batteries. *Angew. Chem. Intern. Ed.* 60, 12931–12940. 10.1002/anie.202101537.
135. Jones, S.D., Nguyen, H., Richardson, P.M., Chen, Y.-Q., Wyckoff, K.E., Hawker, C.J., Clément, R.J., Fredrickson, G.H., and Segalman, R.A. (2022). Design of Polymeric Zwitterionic Solid Electrolytes with Superionic Lithium Transport. *ACS Cent. Sci.* 8, 169–175. 10.1021/acscentsci.1c01260.
136. Babu, H.V., Srinivas, B., and Muralidharan, K. (2015). Design of Polymers with an Intrinsic Disordered Framework for Li-Ion Conducting Solid Polymer Electrolytes. *Polym. Guildf.* 75, 10–16. 10.1016/j.polymer.2015.08.004.
137. Devaux, D., Glé, D., Phan, T.N.T., Gimes, D., Giroud, E., Deschamps, M., Denoyel, R., and Bouchet, R. (2015). Optimization of Block Copolymer Electrolytes for Lithium Metal Batteries. *Chem. Mat.* 27, 4682–4692. 10.1021/acs.chemmater.5b01273.
138. Devaux, D., Liénafa, L., Beaudoin, E., Maria, S., Phan, T.N.T., Gimes, D., Giroud, E., Davidson, P., and Bouchet, R. (2018). Comparison of Single-Ion-Conductor Block-Copolymer Electrolytes with Polystyrene-TFSI and Polymethacrylate-TFSI Structural Blocks. *Electrochimica Acta* 269, 250–261. 10.1016/j.electacta.2018.02.142.
139. Paren, B.A., Nguyen, N., Ballance, V., Hallinan, D.T., Kennemur, J.G., and Winey, K.I. (2022). Superionic Li-Ion Transport in a Single-Ion Conducting Polymer Blend Electrolyte. *Macromolecules* 55, 4692–4702. 10.1021/acs.macromol.2c00459.
140. Nguyen, N., Blatt, M.P., Kim, K., Hallinan, D.T., and Kennemur, J.G. (2022). Investigating Miscibility and Lithium Ion Transport in Blends of Poly(Ethylene Oxide) with a Polyanion Containing Precisely-Spaced Delocalized Charges. *Polym. Chem.* 13, 4309–4323. 10.1039/D2PY00605G.
141. Borzutzki, K., Dong, K., Nair, J.R., Wolff, B., Hausen, F., Eichel, R.-A., Winter, M., Manke, I., and Brunklaus, G. (2021). Lithium Deposition in Single-Ion Conducting Polymer Electrolytes. *Cell Rep. Phys. Sci.* 2, 100496. 10.1016/j.xcrp.2021.100496.
142. Wu, M., Zhang, X., Zhao, Y., Yang, C., Jing, S., Wu, Q., Brozena, A., Miller, J.T., Libretto, N.J., and Wu, T. (2022). A High-Performance Hydroxide Exchange Membrane Enabled by Cu<sup>2+</sup>-Crosslinked Chitosan. *Nat. Nanotechnol.* 17, 629–636. 10.1038/s41565-022-01112-5.
143. Ueno, K., Yoshida, K., Tsuchiya, M., Tachikawa, N., Dokko, K., and Watanabe, M. (2012). Glyme–Lithium Salt Equimolar Molten Mixtures: Concentrated Solutions or Solvate Ionic Liquids? *J. Phys. Chem. B* 116, 11323–11331. 10.1021/jp307378j.
144. Huang, T., Long, M., Wu, G., Wang, Y., and Wang, X. (2019). Poly(Ionic Liquid)-Based Hybrid Hierarchical Free-Standing Electrolytes with Enhanced Ion Transport and Fire Retardancy Towards Long-Cycle-Life and Safe Lithium Batteries. *Chem. Electro. Chem.* 6, 3674–3683. 10.1002/celec.201900686.
145. Jaumaux, P., Liu, Q., Zhou, D., Xu, X., Wang, T., Wang, Y., Kang, F., Li, B., and Wang, G. (2020). Deep-Eutectic-Solvent-Based Self-Healing Polymer Electrolyte for Safe and Long-Life Lithium-Metal Batteries. *Angew. Chem.* 132, 9219–9227. 10.1002/ange.202001793.
146. Chen, D., Zhu, M., Kang, P., Zhu, T., Yuan, H., Lan, J., Yang, X., and Sui, G. (2022). Self-Enhancing Gel Polymer Electrolyte by In Situ Construction for Enabling Safe Lithium Metal Battery. *Adv. Sci.* 9, 2103663. 10.1002/advs.202103663.
147. Lin, Z., Guo, X., Wang, Z., Wang, B., He, S., O'Dell, L.A., Huang, J., Li, H., Yu, H., and Chen, L. (2020). A Wide-Temperature Superior Ionic Conductive Polymer Electrolyte for Lithium Metal Battery. *Nano. Energy* 73, 104786. 10.1016/j.nanoen.2020.104786.
148. Mackanic, D.G., Michaels, W., Lee, M., Feng, D., Lopez, J., Qin, J., Cui, Y., and Bao, Z. (2018). Crosslinked Poly(Tetrahydrofuran) as a Loosely Coordinating Polymer Electrolyte. *Adv. Energy Mater.* 8, 1800703. 10.1002/aenm.201800703.
149. Jeong, D., Shim, J., Shin, H., and Lee, J. (2020). Sustainable Lignin-Derived Cross-Linked Graft Polymers as Electrolyte and Binder Materials for Lithium Metal Batteries. *Chem. Sus. Chem.* 13, 2642–2649. 10.1002/cssc.201903466.
150. Zheng, G., Wang, C., Pei, A., Lopez, J., Shi, F., Chen, Z., Sendek, A.D., Lee, H.-W., Lu, Z., and Schneider, H. (2016). High-Performance Lithium Metal Negative Electrode with a Soft and Flowable Polymer Coating. *ACS Energy Lett.* 1, 1247–1255. 10.1021/acsenrgylett.6b00456.
151. Huang, Z., Choudhury, S., Paul, N., Thienenkamp, J.H., Lennartz, P., Gong, H., Müller-Buschbaum, P., Brunklaus, G., Gilles, R., and Bao, Z. (2022). Effects of Polymer Coating Mechanics at Solid-Electrolyte Interphase for Stabilizing Lithium Metal Anodes. *Adv. Energy Mater.* 12, 2103187. 10.1002/aenm.202103187.
152. Li, N.-W., Shi, Y., Yin, Y.-X., Zeng, X.-X., Li, J.-Y., Li, C.-J., Wan, L.-J., Wen, R., and Guo, Y.-G. (2018). A Flexible Solid Electrolyte Interphase Layer for Long-Life Lithium Metal Anodes. *Angew. Chem. Intern. Ed.* 57, 1505–1509. 10.1002/anie.201710806.

153. Tamwattana, O., Park, H., Kim, J., Hwang, I., Yoon, G., Hwang, T., Kang, Y.-S., Park, J., Meethong, N., and Kang, K. (2021). High-Dielectric Polymer Coating for Uniform Lithium Deposition in Anode-Free Lithium Batteries. *ACS Energy Lett.* *6*, 4416–4425. 10.1021/acsenergylett.1c02224.
154. Wang, X., Zeng, W., Hong, L., Xu, W., Yang, H., Wang, F., Duan, H., Tang, M., and Jiang, H. (2018). Stress-Driven Lithium Dendrite Growth Mechanism and Dendrite Mitigation by Electroplating on Soft Substrates. *Nat. Energy* *3*, 227–235. 10.1038/s41560-018-0104-5.
155. Meng, Y.S., Srinivasan, V., and Xu, K. (2022). Designing better electrolytes. *Science* *378*, eabq3750. 10.1126/science.abq3750.
156. Peled, E., and Menkin, S. (2017). Review—SEI: Past, Present and Future. *J. Electrochem. Soc.* *164*, A1703–A1719. 10.1149/2.1441707jes.
157. Cheng, X.-B., Zhang, R., Zhao, C.-Z., Wei, F., Zhang, J.-G., and Zhang, Q. (2016). A Review of Solid Electrolyte Interphases on Lithium Metal Anode. *Adv. Sci.* *3*, 1500213. 10.1002/advs.201500213.
158. Xu, Y., Dong, K., Jie, Y., Adelhalm, P., Chen, Y., Xu, L., Yu, P., Kim, J., Kochovski, Z., Yu, Z., et al. (2022). Promoting Mechanistic Understanding of Lithium Deposition and Solid-Electrolyte Interphase (SEI) Formation Using Advanced Characterization and Simulation Methods: Recent Progress, Limitations, and Future Perspectives. *Adv. Energy Mater.* *12*, 2200398. 10.1002/aenm.202200398.
159. Wu, L., Nachimuthu, S., Brandell, D., and Jiang, J. (2022). Prediction of SEI Formation in All-Solid-State Batteries: Computational Insights from PCL-based Polymer Electrolyte Decomposition on Lithium-Metal. *Batter. Supercaps* *5*. 10.1002/batt.202200088.

## FIGURE TITLES AND LEGENDS

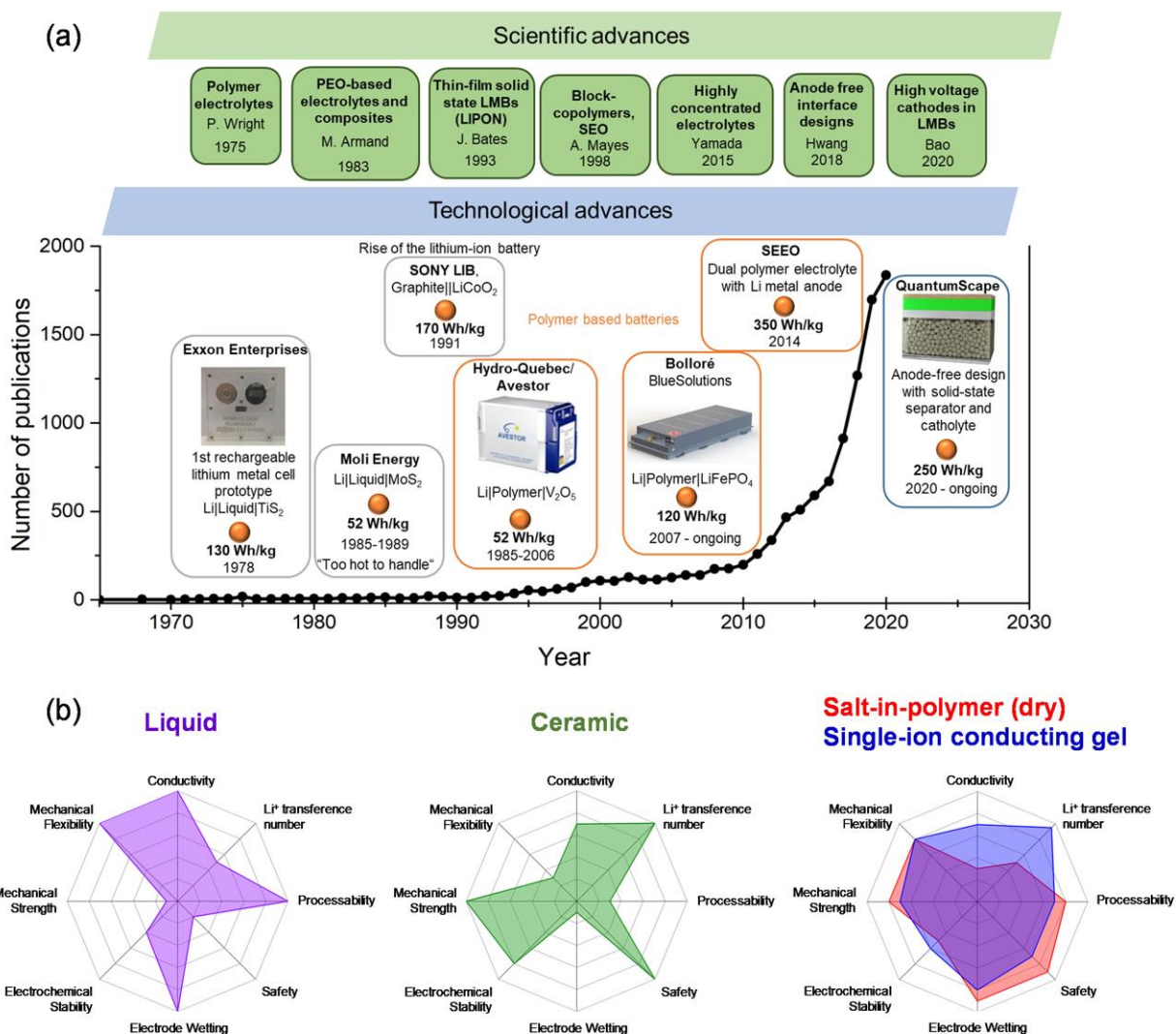


**Figure 1. Scientific milestones and technological advances of lithium metal batteries.**

(a) (top) Selected scientific milestones of rechargeable lithium metal batteries. (bottom) Plot of the number of publications related to “lithium metal anode”, overlaid with some examples of technological advances of LMBs, including their reported gravimetric energy densities. The polymer-based advances have an orange border. Scientific and technological advances were obtained from recent literature: Scientific advances- Polymer electrolytes,<sup>16</sup> PEO-based electrolytes and composites,<sup>16</sup> thin-film solid-state LMBs,<sup>17</sup> SEO block co-polymers,<sup>18</sup> highly concentrated electrolytes,<sup>19</sup> anode free interface designs,<sup>20</sup> high voltage cathodes in LMBs;<sup>20</sup> Technological advances- Li|Liquid|TiS<sub>2</sub> (Exxon Enterprises),<sup>21</sup> Li|Liquid|MoS<sub>2</sub> (Moli Energy),<sup>22</sup> Graphite||LiLiCo<sub>2</sub> (Sony LIB),<sup>23</sup> Li|Polymer|V<sub>2</sub>O<sub>5</sub> (Hydro-Quebec/Avestor),<sup>24</sup>

Li|Polymer,|LiFePO<sub>4</sub> (Blue Solutions),<sup>2,25</sup> Dual Polymer electrolyte with Li metal anode (SEEO),<sup>12</sup> anode free design with solid-state separator and catholyte (QuantumScape)<sup>9</sup> (b) Radar plots comparing key properties of liquid, ceramic, and two classes of polymer electrolytes: traditional dry salt-in-polymer, and single-ion conducting gels. While these plots are qualitative comparisons, examples of ranges of the metrics presented are conductivity: 10<sup>-4</sup>-10<sup>-2</sup> S cm<sup>-1</sup> at 25°C; Li<sup>+</sup> transference number: 0 - 1; Oxidative stability: maximum 5.0 V vs. Li|Li<sup>+</sup>; mechanical strength: elastic modulus of 1-500 GPa.

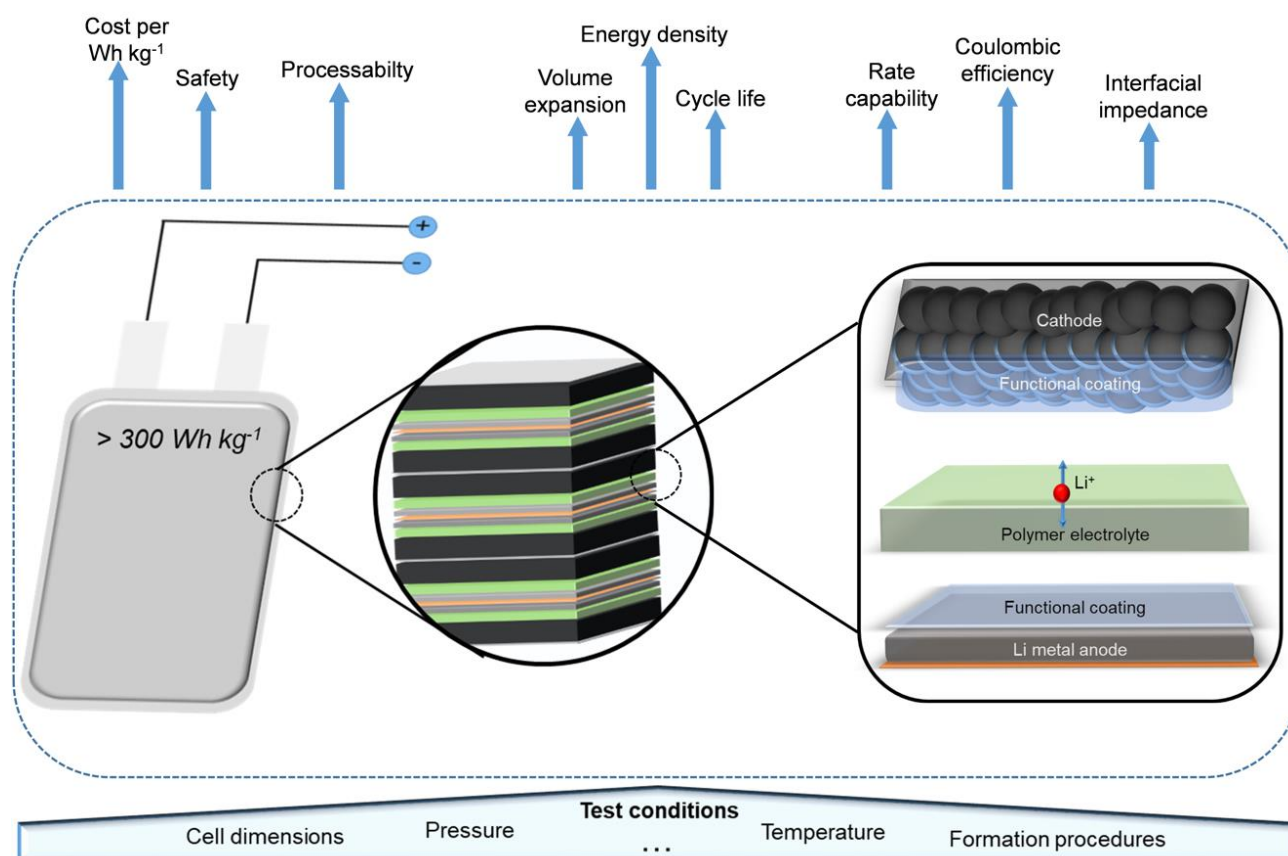


**Figure 2. Key output parameters of lithium metal batteries.**

While each output parameter is important at multiple levels of a battery system, they have been grouped into scales in which they are most often considered or are most relevant. The interaction of these parameters goes beyond the linear scaling of a single cell, and these considerations should be accounted for, when designing a full system.

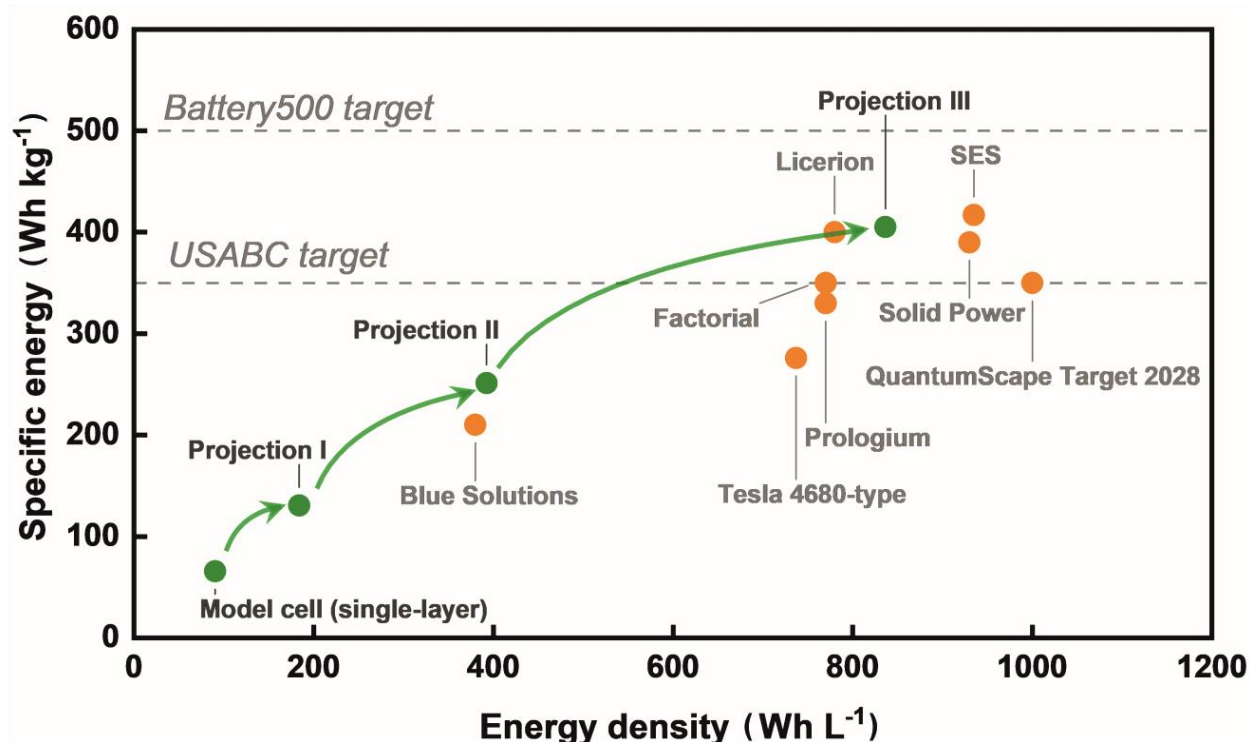


**Figure 3. Projection of specific energy and energy density.**

Projections of a model pouch cell (green) consisting of a lithium metal anode, solid polymer electrolyte and polymer composite cathode, compared to announced target values of commercial manufacturers (orange). The initial academic model cell has a lithium thickness of 50  $\mu\text{m}$ , electrolyte membrane thickness of 50  $\mu\text{m}$ , composite cathode active mass loading of 7  $\text{mg cm}^{-2}$  (60 wt% active material) and a cathode thickness of 65  $\mu\text{m}$ . The cell delivers a reversible discharge capacity of 175  $\text{mAh g}^{-1}$  at 3.5 V. Projection I comprises 15 layers of anode|electrolyte|cathode stacks without any further changes, whereas Projection II has the same number of layers, but a reduced lithium thickness of 20  $\mu\text{m}$ , electrolyte thickness of 25  $\mu\text{m}$ , and thicker cathode (186  $\mu\text{m}$ ) affording a mass loading of 20  $\text{mg cm}^{-2}$  at unchanged voltage and discharge capacity. Projection III consists of a dense and highly loaded cathode (90 % active material, 25  $\text{mg cm}^{-2}$  active mass loading at a thickness of 100  $\mu\text{m}$ ) and delivers a reversible discharge capacity of 200  $\text{mAh g}^{-1}$  at 3.5 V. Further parameters and details of the calculation are provided in the Supporting Information (Table S1). Also shown in the plot for comparison are targets from commercial manufacturers: Blue Solutions,<sup>39</sup> Tesla,<sup>40</sup> Licerion,<sup>41</sup> QuantumScape,<sup>9</sup> Solid Power,<sup>42</sup> SES,<sup>43</sup> Prologium,<sup>44</sup> and Factorial.<sup>45</sup>



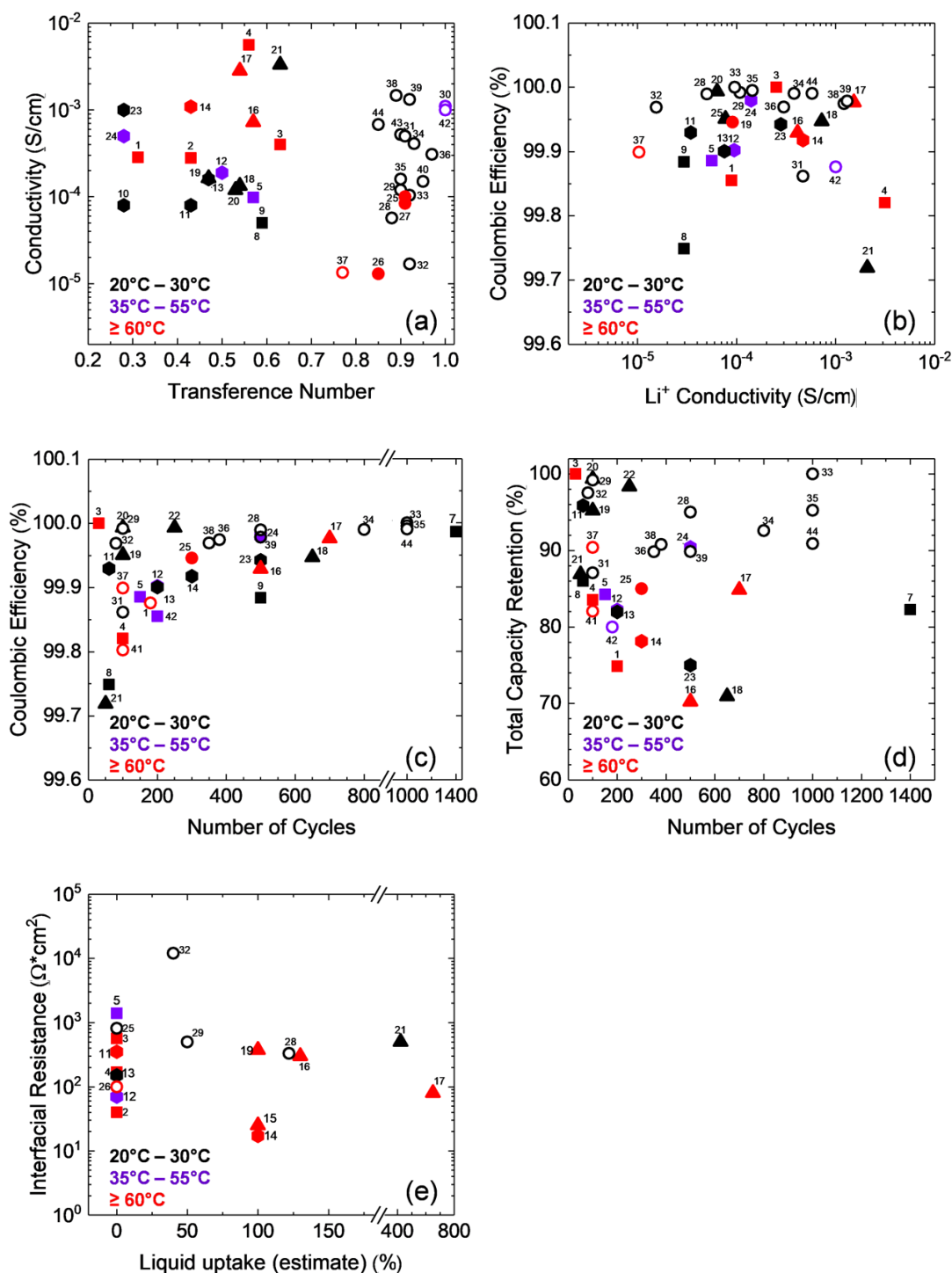


**Figure 4. Electrochemical data for single-cell lithium metal batteries operated with polymer electrolytes.**

(a) Conductivity vs. transference number (b) (Cathode) Coulombic Efficiency vs. Li<sup>+</sup> Conductivity. (c) (Cathode) Coulombic Efficiency vs. number of cycles reported (d) capacity retention vs. number of cycles reported (e) Area interfacial/interphasial resistance vs. liquid



uptake. The electrolytes are labeled as: ■ polymer + Li-salt<sup>25,75,76,78–81</sup> (index 1-9); ● polymer ceramic composite + Li-salt<sup>60,82–85</sup> (index 10-14); ▲ polymer gel + Li-salt<sup>86–92</sup> (index 15-24); ● Dry SIC<sup>93–95</sup> (index 25-27); ○ SIC gels<sup>61,96–110</sup> (index 28-44). The data are from selected references from Table S2, and the label on each point is the index number from Table S2. References were used if the plotted data was reported. Points are **black** if data was collected at room temperature (20 – 30 °C), **purple** if the data was collected between 35 – 55 °C, and **red** if data was collected ≥ 60 °C. The presented Coulombic efficiency was calculated from the available data of cycle number and capacity retention at the end of cycling, as other representations of cycling efficiency, such as accumulated Coulombic efficiency,<sup>111</sup> could not be extracted from most references.

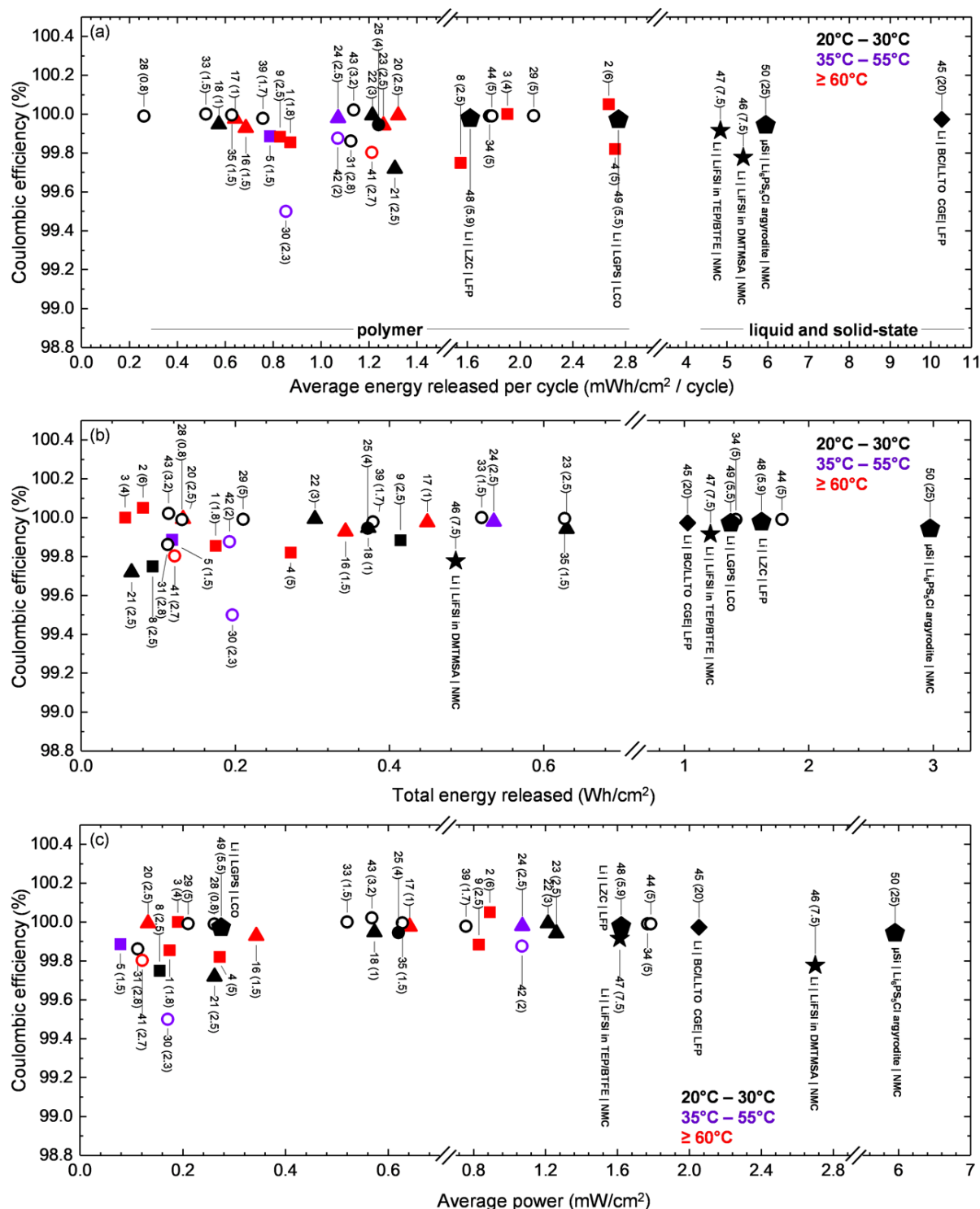


**Figure 5. Critical data comparison of various cell chemistries.**

Average (cathode) Coulombic efficiency vs. (a) average energy released per cycle, (b) total energy released during cycling, and (c) average power for different polymer electrolytes in single-cell LMB full cells in literature (index 1-44). The electrolytes are labeled as: ■ polymer + Li-salt; ▲

polymer gel + Li-salt; ● Dry SIC; ○ SIC gels. Each point is also labeled with the index from Table S2, with the active mass loading of the cathode (units of  $\text{mg cm}^{-2}$ ) in parenthesis. The data is from select references from Table S2. References were used if all necessary metrics required to calculate average energy released per cycle were reported. Recently developed liquid (★), solid-state (◆), and a combined ◆ liquid/ceramic/polymer electrolyte data is presented for comparison (index 45-50): LiFSI in DMTMSA,<sup>7</sup> LiFSI in TEB/BTFE,<sup>6</sup> a system with a Li anode and LZC solid-state electrolyte,<sup>13</sup> a system with a Li anode and LGPS solid-state electrolyte,<sup>14</sup> a system based on a Si-anode and a  $\text{Li}_6\text{PS}_5\text{Cl}$  solid-state electrolyte,<sup>8</sup> and a cellulose based aerogel, with LLZO nanowires and  $\text{LiPF}_6$  in EC/DMC.<sup>115</sup> Points are **black** if data was collected at room temperature (20 – 30 °C), **purple** if the data was collect between 35 – 55 °C, and **red** if data was collected  $\geq 60$  °C. We note that the presented Coulombic efficiency is an average value based on the available data, other representations of cycling efficiency, such as accumulated Coulombic efficiency<sup>111</sup> or lithium figure of merit,<sup>113,114</sup> could not be extracted from most literature references.

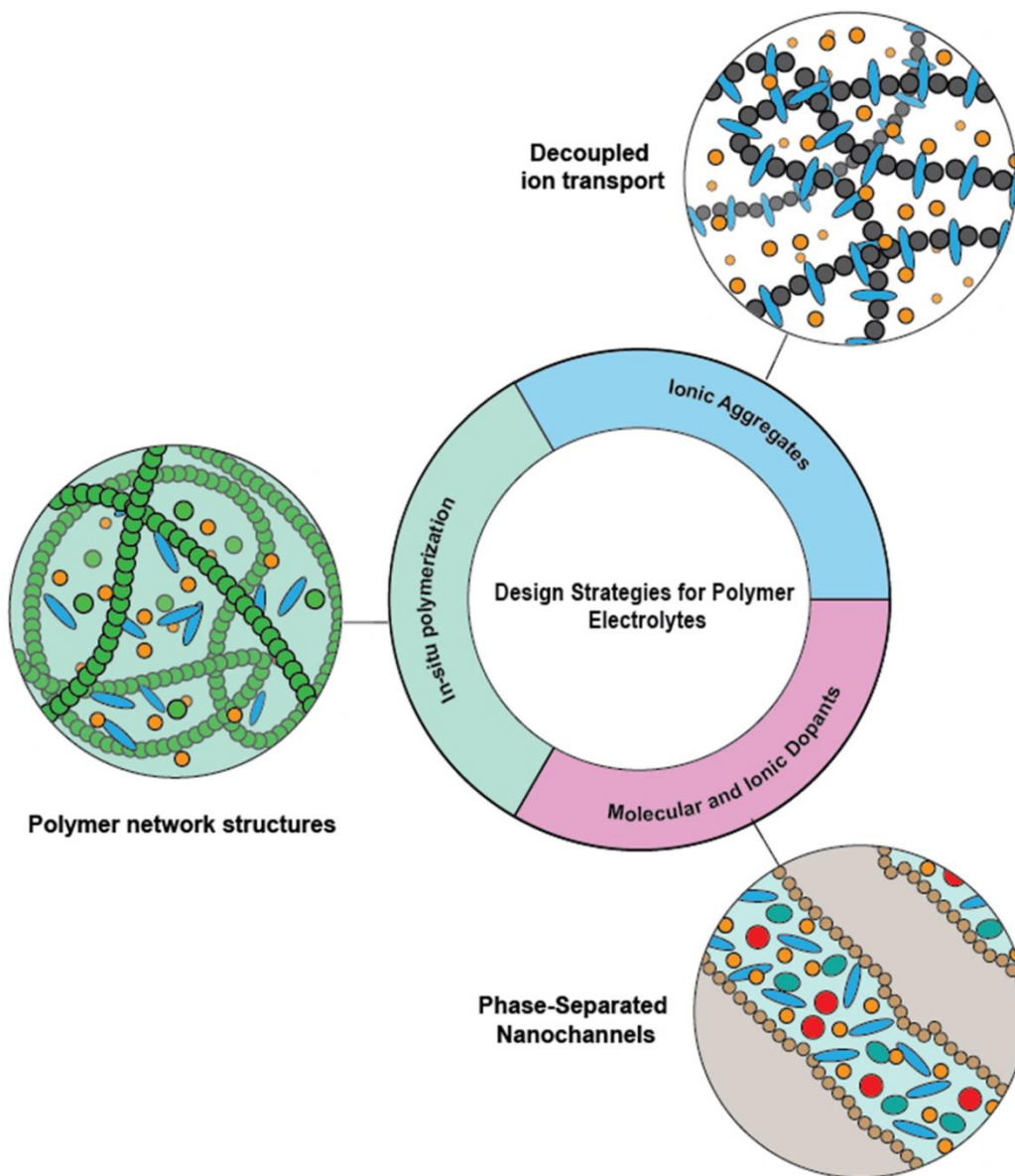


**Figure 6. Design strategies for polymer electrolytes.**

Schematic illustrations highlighting design strategies for polymer electrolytes, including polymer network structures, decoupled ion transport and phase-separated nanochannels.

## Polymer electrolytes & Li metal

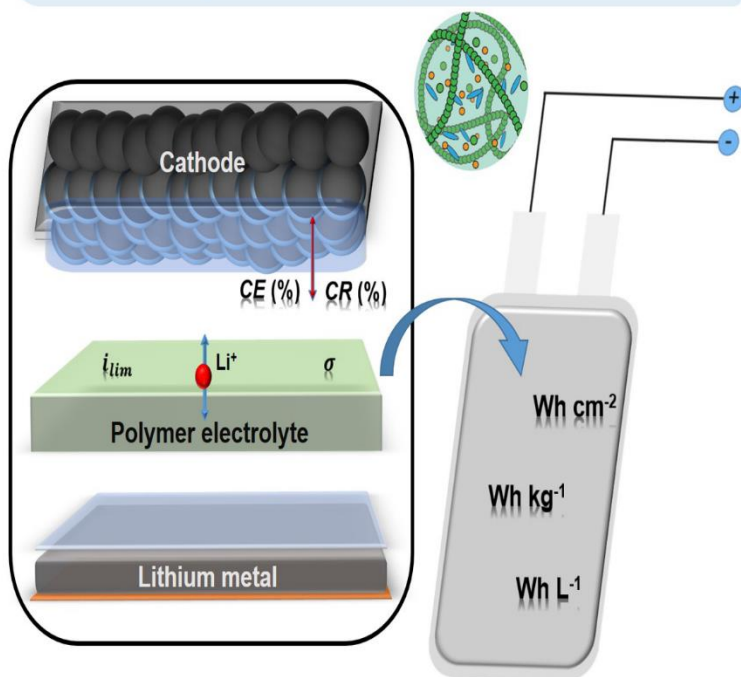


**Table 1. Select parameters of single-cell LMBs and polymer electrolyte properties.**

The data was collected from the literature, ranges are the maximum and minimum values reported in references listed in **Table S2** (Index 1-44).

Parameter	Range
Cathode mass loading	0.8 – 23 $\text{mg cm}^{-2}$
Lithium thickness	20 – 500 $\mu\text{m}$
Initial specific capacity	80 – 270 $\text{mAh g}^{-1}$
Voltage window	3.2 – 3.9 V
Cycle number shown	8 – 1400
Operating temperature	20 – 100 $^{\circ}\text{C}$
Ionic conductivity	$10^{-5}$ – $10^{-2}$ $\text{S cm}^{-1}$
$\text{Li}^+$ transference number	0.25 – 1